



Picture taken at SPE  
ACCE (Automotive  
composites conference  
and exhibition) 2018

# 2017-2018 The Baylor SPE Chapter The year in review



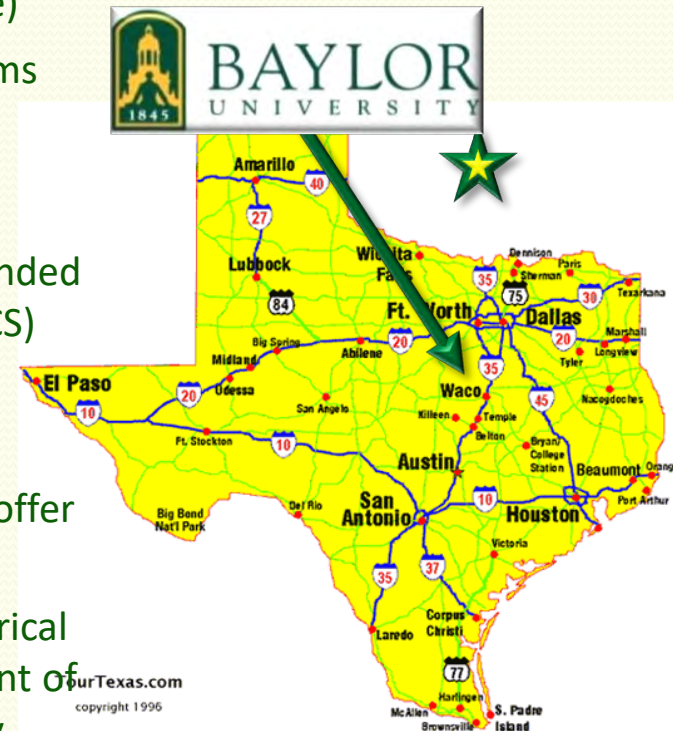


BAYLOR  
UNIVERSITY

# Baylor University



- Baylor University was chartered in 1845 by the Republic of Texas under the mission of Pro Ecclesia and Pro Texana
- Baylor has an enrollment of 17,000 students (14,300 undergraduate)
- Baylor has 142 undergraduate, 75 master's, and 42 doctoral programs
- Student to faculty ratio is 15 to 1 across the campus
- Baylor's School of Engineering and Computer Science (ECS) was founded in 1995 with two departments, Department of Computer Science (CS) and Department of Engineering
- The only graduate degree in 1995 was an M.S. in Computer Science
- The Department of Engineering was granted permission in 2004 to offer master's degrees
- In 2006 the Departments of Mechanical Engineering (ME) and Electrical and Computer Engineering (ECE) were formed out of the Department of Engineering. Currently the two departments have 14 and 16 faculty, respectively
- Dean Dennis O'Neal, has spearheaded the growth of the research programs in the school
- In 2017 Sarah Stair (an SPE member and former president) graduated as the first mechanical engineering Ph.D.





BAYLOR  
UNIVERSITY

# Baylor University



- There are 1,106 undergraduate students in ECS (2015-2016), with 5,100 new applications for the fall of 2014 (double that of 5 years ago)
- The student body in ECS is composed of 25% female and 30% minority
- ~80 graduate students in ECS, with ~40 of those in ME
- The materials group (self labeled Sic'em – Scientific Innovations in Complex Engineering Materials) has moved to the BRIC (Baylor Research Innovation Corporate) in 2013.
- Currently Sic'em has 4,600 sq. ft. of lab and office space
- Materials faculty have received funding from NSF, NASA, AFOSR, ONR, L-3 Communications, Hess Inc., Delta G, Sandia National Laboratory, Oak Ridge National Laboratory, DOE (Education), Leggett and Platt, the Kern Foundation and Axion Structural Innovations.







# SPE Equipment

- Filabot
- Benchtop Injection Molder
- Solidoodle
- Carvey
- Vacuum Pump and resin trap
- Brabender Mixer
- Various material supplies







BAYLOR  
UNIVERSITY

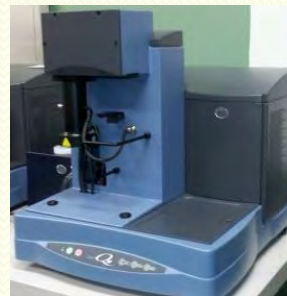
# Available Equipment

## Imaging

- JEOL JSM Scanning Electron Microscope with 5,000 N tensile stage
- Panametrics 300 gallon, 200 MHz 3 ft x 4 ft x 6 ft NDT Immersion System
- Keyence VR-3200 – high resolution 3D, non-contact, surface measurements
- Custom C-Scan Immersion System, 5 - 25 MHz, 1/800<sup>th</sup> mm x-y-z resolution, 0.01° resolution in rotation stage
- Custom C-Scan Out-of-tank System, 5 - 25 MHz, 1/800<sup>th</sup> mm x-y resolution
- Leica binocular/stereo microscope
- MZ7 Microzoom 10x-1000x magnification, 10 MP video imaging
- Multiple Dino-Lite Polarizing portable microscopes
- Non-contact 3D digitizer/scanner – NextEngine 3D

## Materials Fabrication/Processing

- K-Lab Magnetron sputter system for Thin Film Electronic/Flexible Polymers
- Multiple vacuum pump systems (VARTM) for fabricating laminated composites
- CTE M7000 Constant Speed Mixer, API Spec 10
- ExOn 8, 12 lb/hr extruder with custom translation system for large volume additive manufacturing
- Custom CVD chamber for nanotube synthesis
- Arburg 70 ton injection molding machine with 5 molds
- Brabender single screw extruder
- Ross mixing unit
- Carbolite split tube furnace for MWNT CVD fabrication
- DSM X-Plore Injection molding machine
- Makerbot Replicator 2 and 2x, and SolidDoodle 3D Printers
- Objet and Dimension 3D printers (dept. resource)
- Compression molding 60 ton hot press
- CNC with 4 axis capability (dept. resource)





# Available Equipment

## Materials Characterization

- TA Instruments DMA Q800 – Dynamic Mechanical Analyzer
- TA Instruments TGA Q50 – Thermogravimetric Analyzer
- TA Instruments M/DSC Q20 – Differential Scanning Calorimeter
- TA Instruments Q400 TMA – Thermomechanical Analyzer
- Malvern Bohlin Gemini II Rheometer
- Instron CEASt 9050 Charpy and Izod Impact Testor
- Desktop Instron with 10lb and 450lb cells
- Test Resources 810LE Tensile Stage – 15 kN static, 8.5 kN dynamic @ 15Hz
- MTS Qtest/100, 100kN tensile test load frame
- Custom 8 foot drop tower with 1 to 25 pound load tray
- Tinius Olsen Meltflow Indexer – MP600



## Sample Preparation and Measurement Devices

- Blue M LO-225 Programmable Oven – Interior Dims. 24" x 20" x 30"
- Plasma Etch PE50-HF
- Buehler EcoMet Grinder-Polisher and Buehler IsoMet Low Speed Saw
- Multiple National Instruments Data Acquisition cards and chassis
- Agilent Oscilloscopes and Programmable Power Supplies



## Computational Resources

- Twelve high performance workstations (most are Intel i7 or Xeon 8-core), each 3.06 GHz or higher, with 32, 64 or 256 GB of ram
- 6 node portable desktop cluster, 12 cores, CUDA cards
- Full access to Baylor's HPC with 128 nodes of dual Xeon 5355s with 16 GB ram per blade (Baylor resource)
- 5 standard fume hoods (2 – 48" width, 2 – 60" width, 1 – 72" width) and one highly acidic fume hood with ultrafine (SWNT scale) particle filtration

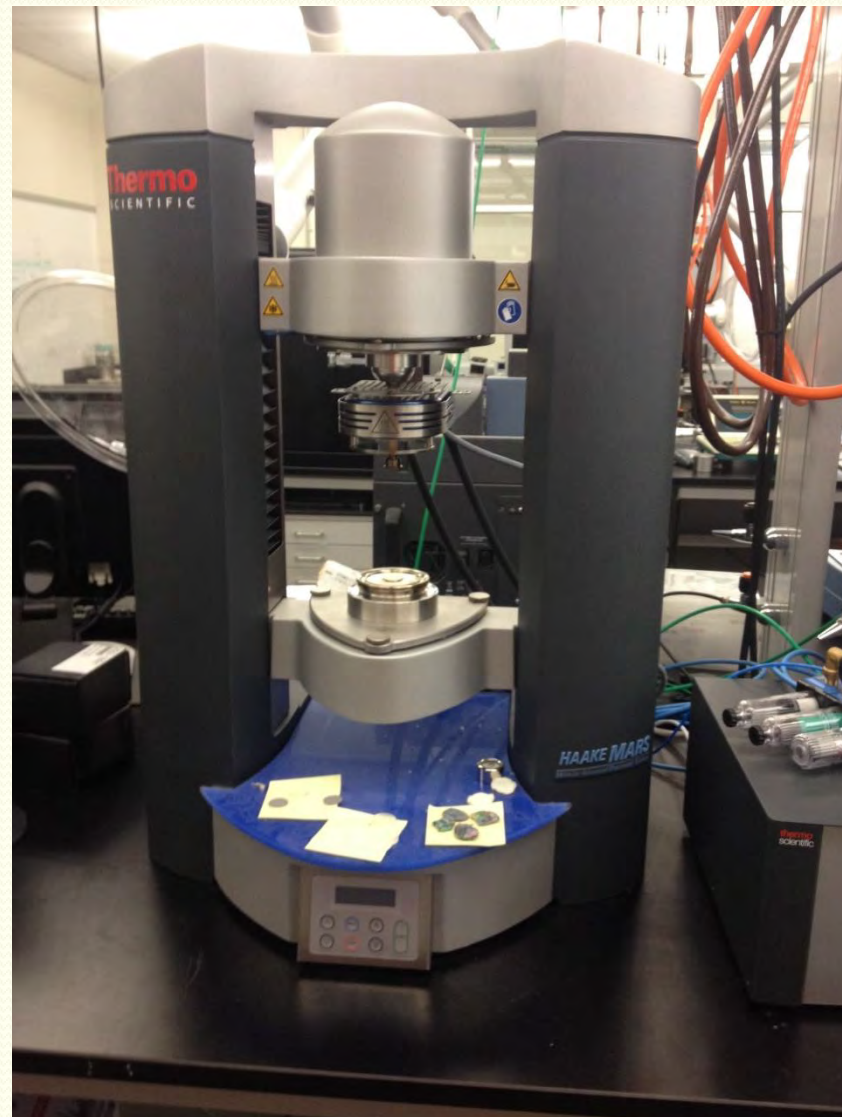
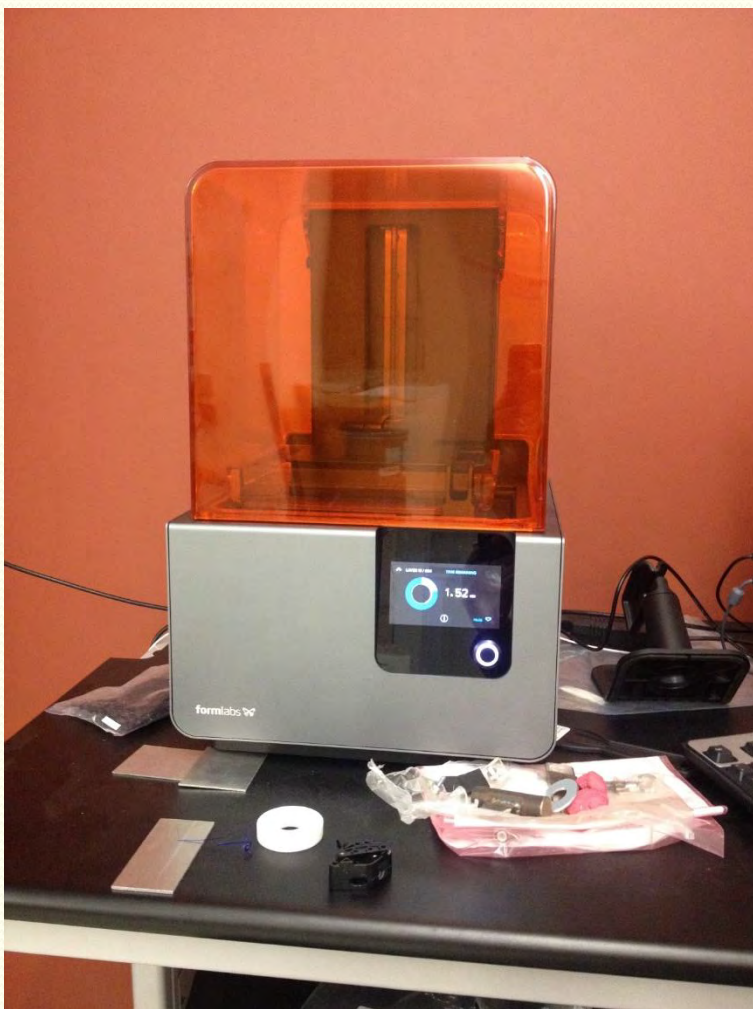






# SPE Equipment - 2017

- Form 2 SLA 3D Printer
- Thermo Scientific Rheometer



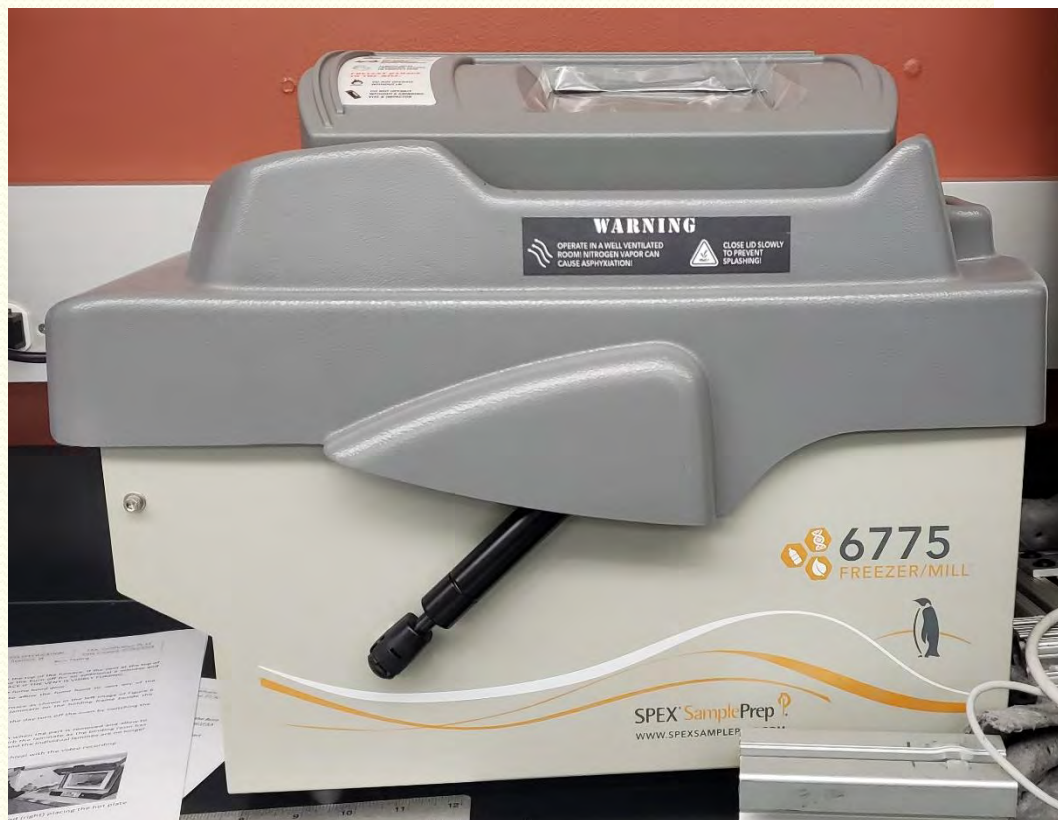


BAYLOR  
UNIVERSITY

# SPE Equipment Purchased - 2018



- Freezer/Mill 6775
- Vertical Mill with Powerfeed & DRO





# The Baylor SPE Chapter 2017-2018

## The year in review





# Student Officers

**Daniel Pulipati**

**President  
2017 - 2018**



**Daniel Pulipati**

**President  
2018 - 2019**



**Jay Thomas**

**Vice President  
2017 - 2018**



**Nate Blackman**

**Vice President  
2018 - 2019**



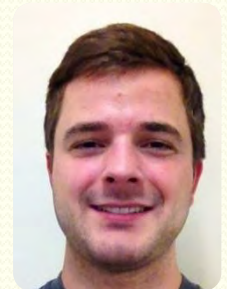
**John Moreton**

**Treasurer  
2017 - 2018**



**Timothy Russell**

**Treasurer  
2018 - 2019**



**Evan Wang**

**Secretary  
2017 - 2018**



**Dale Jiang**

**Secretary  
2018 - 2019**







BAYLOR  
UNIVERSITY

# Faculty Members in Polymers, and Composites



**Dr. William Jordan**

**Professor and Chair  
of Mechanical  
Engineering**



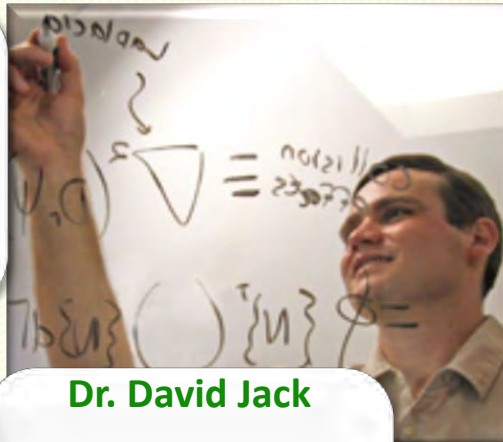
**Dr. Douglas E. Smith**

**Associate Professor  
of Mechanical  
Engineering**



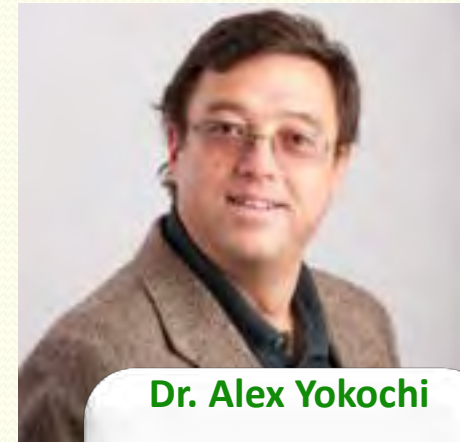
**Dr. Sunghwan Lee**

**Assistant Professor  
of Mechanical  
Engineering**



**Dr. David Jack**

**Associate Professor  
of Mechanical  
Engineering**



**Dr. Alex Yokochi**

**Professor of  
Mechanical  
Engineering**



BAYLOR  
UNIVERSITY

# Student Members



- 25 current members
- 1 Post Doc
- 1 Facility Advisor
- 15+ Alumni







# SPE Chapter and Member Awards



- Evan Wang received 1<sup>st</sup> place in the Graduate Student Poster Competition at the 2017 SPE-ACCE meeting
- Ben Blandford received the ACCE scholarship award in 2017.
- Ben Blandford also received the Harold Giles Award winner in 2017.
- Evan Wang received travel award for ANTEC 2017.
- Evan Wang also won the scholarship award at the Polyolefins conference 2018.



Evan Wang

Ben Blandford



BAYLOR  
UNIVERSITY

# Best Faculty Advisor – Baylor



Dr. David Jack won the best faculty advisor award among all the student organization advisors at Baylor.



BAYLOR  
UNIVERSITY

# SPE Outstanding Student Chapter



- The Outstanding Student Chapter of the Year award seeks to recognize the top student SPE chapters each year that have demonstrated true excellence in the proliferation of plastics engineering education.
- Baylor's SPE chapter received 2<sup>nd</sup> place for SPE Outstanding Student Chapter of the Year Award (out of all SPE student organizations). Baylor's SPE chapter was placed as top three SPE student organizations every year since formation - 2018.





# Monthly Guest Speakers



# Society of Plastics Engineers (SPE) Meeting

Come join SPE as we host **Dr. David Jack**,  
Baylor Mechanical Engineering professor. **He**  
**will be discussing an overview of materials**  
**research at Baylor University and the**  
**department of Mechanical Engineering with**  
**Hands on demonstrations.**



**Thursday, Sep 14<sup>th</sup>**

**6:30 p.m.**

**Rogers 106**

**FREE PIZZA and SODA**

# Society of Plastics Engineers (SPE) Meeting

Come join SPE as we host **Mr. Don Roberts**,  
from **Lockheed Martin**. He will be discussing  
some of his experience in Aeronautics and  
helping students to navigate in getting hired  
at Lockheed Martin.



LOCKHEED MARTIN

BAYLOR  
SPE

ASME

LOCKHEED MARTIN

**LOCKHEED MARTIN  
INFO SESSION**

THURSDAY, OCTOBER 19TH  
6:30-8:00 PM  
ROGERS 109

Food provided!

TO REACH GREAT HEIGHTS, START WITH A GREAT PURPOSE

100  
YEARS OF  
ACCELERATING  
TOMORROW

**Thursday, Oct 16<sup>th</sup>**

**6:30 p.m.**

**Rogers 109**

**FREE PIZZA and SODA**



# Society of Plastics Engineers (SPE) Meeting

Come join SPE as we host **Dr. Valerie Thomas**, from **Georgia Tech University** as she will be discussing on “**Plastics: The immense, Eternal Footprint Humanity Leaves on Earth**”.

**Plastics: The Immense, Eternal Footprint Humanity Leaves on Earth**

## **Dr. Valerie Thomas**

Plastics have been in the news, and the news is not positive. The talk title is a quotation from a newspaper headline from July 2017, reporting on a widely cited study. Moreover, recycling rates are low, and it's not always clear that recycling plastics is beneficial. The talk will draw on recent research, assessments, and publications to provide an eclectic overview of costs, benefits, and challenges of recycling and managing plastics.

Valerie Thomas is the Anderson Interface Professor of Natural Systems at the Georgia Institute of Technology, with appointments in the School of Industrial and Systems Engineering and in the School of Public Policy.



**Thursday, Nov 16<sup>th</sup>**

**6:30 p.m.**

**Rogers 106**

**FREE PIZZA!**

**FREE PIZZA and SODA**

# Society of Plastics Engineers (SPE) Meeting

SPE will be hosting **Jennifer Latiolais** this Thursday for a presentation on **Injection Molding with an emphasis on Scientific Molding.**



**Thursday, January 25<sup>th</sup>**

**6:30 p.m.**

**Rogers 106**

**FREE PIZZA and SODA**



# Society of Plastics Engineers (SPE) Meeting

SPE will be hosting Rick Pardun from L3 communications also the co founder of Maker's Edge Makerspace this Thursday for a presentation on Plastics in Aircraft interiors and how learning different processes can be an edge in job search.



**Thursday, February 20<sup>th</sup>**

**6:30 p.m.**

**Rogers 207**

**FREE PIZZA and SODA**

# Society of Plastics Engineers (SPE) Meeting

SPE will be hosting **Kelsi Mcghee from L3** this Thursday. She will be discussing her experience in **Munitions Directorate of the Air Force Research Lab** doing weapons engineering (design/test) and on a weaponized military aircraft project.



**Tuesday, March 20<sup>th</sup>**

**6:30 p.m.**

**Rogers 106**

**FREE PIZZA and SODA**



# Society of Plastics Engineers (SPE) Meeting

SPE will be hosting **Dr. Alex Yokochi** this Thursday for a presentation on **advanced materials and energy solutions.**



**Thursday, April 19<sup>th</sup>**

**6:30 p.m.**

**Rogers 106**

**FREE PIZZA and SODA**

# Facility Tours and Equipment Demonstrations





# Site Visit – All Plastics

- All Plastics has their corporate office and a manufacturing plant in Dallas and San Antonio, Texas. They are involved in Pharmaceuticals, Industrial, Medical, packaging and consumer products.
- Students were able to tour the facility and see injection molding, automation, scientific molding as well as the product testing.







# Site Visit – Exxon Mobil

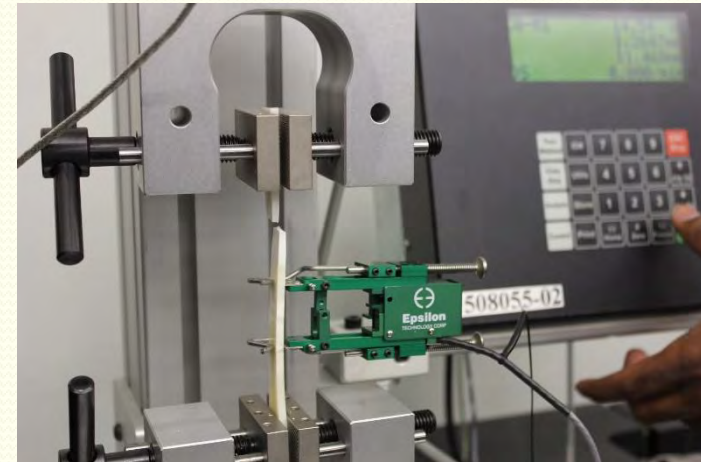
- ExxonMobil's state-of-the-art campus north of Houston serves as home to its Upstream, Downstream, Chemicals and XTO Energy companies and their associated service groups. The facility opened in 2014 and accommodates more than 10,000 employees and visitors.
- Students were able to tour their work area's, talk to Industry experts as well as recruitment officers.





# Injection Molding and Tensile Testing

- Students learned the mold flow index machine, injection molding machines and Tensile testing as a part of equipment demonstrations.





# Student Posters and Presentations Given at SPE Conferences







# Conference Attendance – ACCE



- Students attended the Automotive Composites Conference and Exhibition in Novi, Michigan in the Fall of 2017. Students were able to interact with industry professionals and present their work.
- We had 7 poster presentations
- We had 2 podium presentations

Evan Wang received 1<sup>st</sup> place  
in the graduate student  
poster competition





SEPT 6-8 2017

# Composites: Solutions for a Multi-Material World



## ACCE Poster



## The Effect of Polymer Melt Rheology on Predicted Die Swell and Fiber Orientation in Fused Filament Fabrication (FFF) Nozzle Flow



Zhaogui Wang, PhD Candidate, Research Assistant  
Douglas E. Smith, PhD, PE, Associate Professor

Baylor University  
Mechanical Engineering Department

**Background**  
The Oak Ridge National Laboratory (ORNL) and their associated collaborators are working to evolve the FFF from small scale rapid prototyping to large scale manufacturing for parts and tooling [1]. To achieve high dimensional accuracy and other improved mechanical properties, carbon fiber filled polymers are extremely used.



FIGURE 1. Large Scale FFF Printing System (Courtesy of ORNL)

**Motivation**  
The orientation of short carbon fibers suspended in FFF polymers is highly dependent on the velocity flow field during extrusion, especially when large scale deposition processes are investigated. Previous literature has shown that the flow-induced fiber orientation is a pivotal factor in determining the mechanical properties of solidified parts made by additive based manufacturing process.

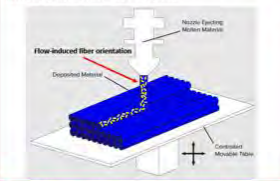


FIGURE 2. Representation of flow-induced fiber orientation associated with FFF process [2]

- Q & A**
- What is the pattern of flow-induced fiber orientation in the flow extrudate?
    - The fiber orientation is significantly influenced by the flow kinematics.
  - How to compute fiber orientation using the flow kinematics?
    - Decoupled fiber orientation from velocity [7] solves the fluid flow problem as if the fibers were not present, then use flow kinematics to compute the fiber orientation. This method has been proved to be effective for shear dominated narrow gap flows (i.e. injection molding) [7].
    - AdvanTucker fiber orientation tensor model has been used in the decoupled model for fiber orientation evaluation [8].
  - How to obtain the flow kinematics of the melt flow?
    - ANSYS Polyflow [3] is a well-validated finite element suite, which is especially robust for polymer process simulation.
  - Predictions using non-Newtonian fluid (i.e. viscoelastic polymer melt) exhibit die swell which has a significant effect on fiber orientation.

ANSYS Polyflow

### Conclusions

- Shear thinning of polymer melts reduces die swell effect.**
  - Die swell using GNF model Cross law is **30.5% less** than using Newtonian model (in LLDE case).
- Viscoelasticity of polymer melts enhances die swell effect.**
  - Die swell using PTT model is **72.2% more** than using Newtonian model (in LLDE case).
- Decouple fiber orientation tensor model is viable.**
  - PTT model yields **lower** principal alignment results than those from GNF models (in LLDE case).

### ABSTRACT

- Extrudate swell** during FFF polymer extrusion was evaluated using selected non-Newtonian fluid rheology models (i.e. Power law model, Cross law model, and Phan-Thien-Tanner Model).
- Flow-induced fiber orientation** state associated with the FFF nozzle flow was computed using AdvanTucker fiber orientation tensors and IRD diffusion from the flow kinematics computed with the rheology models.

#### Objectives

- Formulate a numerical approach to characterize the interaction between the polymer melt flow and concentrated fiber suspensions.
- As preliminary stage, solve the flow induced fiber orientation using decoupled model

#### Large Scale FFF System

- Stratagress Model 3D printing extruder [4]. Flow rate up to 20 ft<sup>3</sup>/hour
- One dimensional gantry system currently, the 3D system under development
- Available Resin: 170, 180, 190, 200, 210, 220, 230, 240, 250, 260, 270, 280, 290, 300, 310, 320, 330, 340, 350, 360, 370, 380, 390, 400, 410, 420, 430, 440, 450, 460, 470, 480, 490, 500, 510, 520, 530, 540, 550, 560, 570, 580, 590, 600, 610, 620, 630, 640, 650, 660, 670, 680, 690, 700, 710, 720, 730, 740, 750, 760, 770, 780, 790, 800, 810, 820, 830, 840, 850, 860, 870, 880, 890, 900, 910, 920, 930, 940, 950, 960, 970, 980, 990, 1000



FIGURE 3. Large Scale FFF Printing System (Courtesy of ORNL)

#### Numerical Modeling FFF Nozzle Flow

Experiments show a significant amount of die swell for the neat ABS feedback (see FIGURE 4-a).



FIGURE 4. (a) Extrudate swell of ABS at the 3D printing system. (b) Geometry of the nozzle

- Based on the geometry of the nozzle, we create a 3D axisymmetric Stokes flow model for the flow domain that includes flow in the nozzle and beyond the nozzle exit. Note, this would save computational time significantly.

FIGURE 5. Flow domain used in the ANSYS Polyflow. The extruded boundary condition was applied to the exit.

#### Extrudate Swell Prediction

Gargy et al. [5] performed a die swell simulation of the LLDE and LLDE by fitting the polymer melt flow with the Carreau-Yasuda flow model. Phan-Thien-Tanner (PTT) for preliminary tests, we used the material properties of LLDE (poly) in their paper [5] in order to approximately formulate our calculation for polymer die swell. However, we are aware that LLDE is not a conventional printable material for FFF process especially in large scale applications.

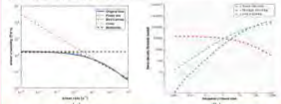


FIGURE 6. (a) Extrudate swell ratio of polymer melt, (b) extrudate swell ratio of polymer melt, (c) extrudate swell ratio of polymer melt, (d) extrudate swell ratio of polymer melt, (e) extrudate swell ratio of polymer melt, (f) extrudate swell ratio of polymer melt, (g) extrudate swell ratio of polymer melt, (h) extrudate swell ratio of polymer melt, (i) extrudate swell ratio of polymer melt, (j) extrudate swell ratio of polymer melt, (k) extrudate swell ratio of polymer melt, (l) extrudate swell ratio of polymer melt, (m) extrudate swell ratio of polymer melt, (n) extrudate swell ratio of polymer melt, (o) extrudate swell ratio of polymer melt, (p) extrudate swell ratio of polymer melt, (q) extrudate swell ratio of polymer melt, (r) extrudate swell ratio of polymer melt, (s) extrudate swell ratio of polymer melt, (t) extrudate swell ratio of polymer melt, (u) extrudate swell ratio of polymer melt, (v) extrudate swell ratio of polymer melt, (w) extrudate swell ratio of polymer melt, (x) extrudate swell ratio of polymer melt, (y) extrudate swell ratio of polymer melt, (z) extrudate swell ratio of polymer melt

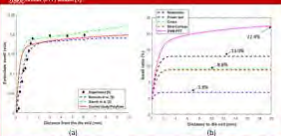


FIGURE 7. (a) Extrudate swell ratio of polymer melt, (b) extrudate swell ratio of polymer melt, (c) extrudate swell ratio of polymer melt, (d) extrudate swell ratio of polymer melt, (e) extrudate swell ratio of polymer melt, (f) extrudate swell ratio of polymer melt, (g) extrudate swell ratio of polymer melt, (h) extrudate swell ratio of polymer melt, (i) extrudate swell ratio of polymer melt, (j) extrudate swell ratio of polymer melt, (k) extrudate swell ratio of polymer melt, (l) extrudate swell ratio of polymer melt, (m) extrudate swell ratio of polymer melt, (n) extrudate swell ratio of polymer melt, (o) extrudate swell ratio of polymer melt, (p) extrudate swell ratio of polymer melt, (q) extrudate swell ratio of polymer melt, (r) extrudate swell ratio of polymer melt, (s) extrudate swell ratio of polymer melt, (t) extrudate swell ratio of polymer melt, (u) extrudate swell ratio of polymer melt, (v) extrudate swell ratio of polymer melt, (w) extrudate swell ratio of polymer melt, (x) extrudate swell ratio of polymer melt, (y) extrudate swell ratio of polymer melt, (z) extrudate swell ratio of polymer melt

**Fiber Orientation Computation**  
We compute the fiber orientation of the nozzle flow using the AdvanTucker tensor model [5] and Ffowkes-Young [6] orientation diffusion. Since polymer melt is extruded along a direction, the flow of the orientation tensor will be put on the  $\hat{e}_1$  component of the 2<sup>nd</sup> order orientation tensor, which indicates how well the fibers would align along extruding direction.

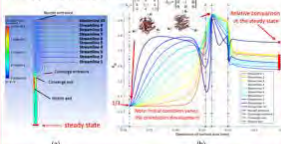


FIGURE 8. (a) Fiber orientation tensor components of polymer melt, (b) fiber orientation tensor components of polymer melt, (c) fiber orientation tensor components of polymer melt, (d) fiber orientation tensor components of polymer melt, (e) fiber orientation tensor components of polymer melt, (f) fiber orientation tensor components of polymer melt, (g) fiber orientation tensor components of polymer melt, (h) fiber orientation tensor components of polymer melt, (i) fiber orientation tensor components of polymer melt, (j) fiber orientation tensor components of polymer melt, (k) fiber orientation tensor components of polymer melt, (l) fiber orientation tensor components of polymer melt, (m) fiber orientation tensor components of polymer melt, (n) fiber orientation tensor components of polymer melt, (o) fiber orientation tensor components of polymer melt, (p) fiber orientation tensor components of polymer melt, (q) fiber orientation tensor components of polymer melt, (r) fiber orientation tensor components of polymer melt, (s) fiber orientation tensor components of polymer melt, (t) fiber orientation tensor components of polymer melt, (u) fiber orientation tensor components of polymer melt, (v) fiber orientation tensor components of polymer melt, (w) fiber orientation tensor components of polymer melt, (x) fiber orientation tensor components of polymer melt, (y) fiber orientation tensor components of polymer melt, (z) fiber orientation tensor components of polymer melt

**Future Work**

- Simulate printable material (i.e. ABS, CF-ABS) using our algorithm
- Light computational viscoelastic model
- Coupled Formulation / Non-Newtonian analysis (see FIGURE 8)

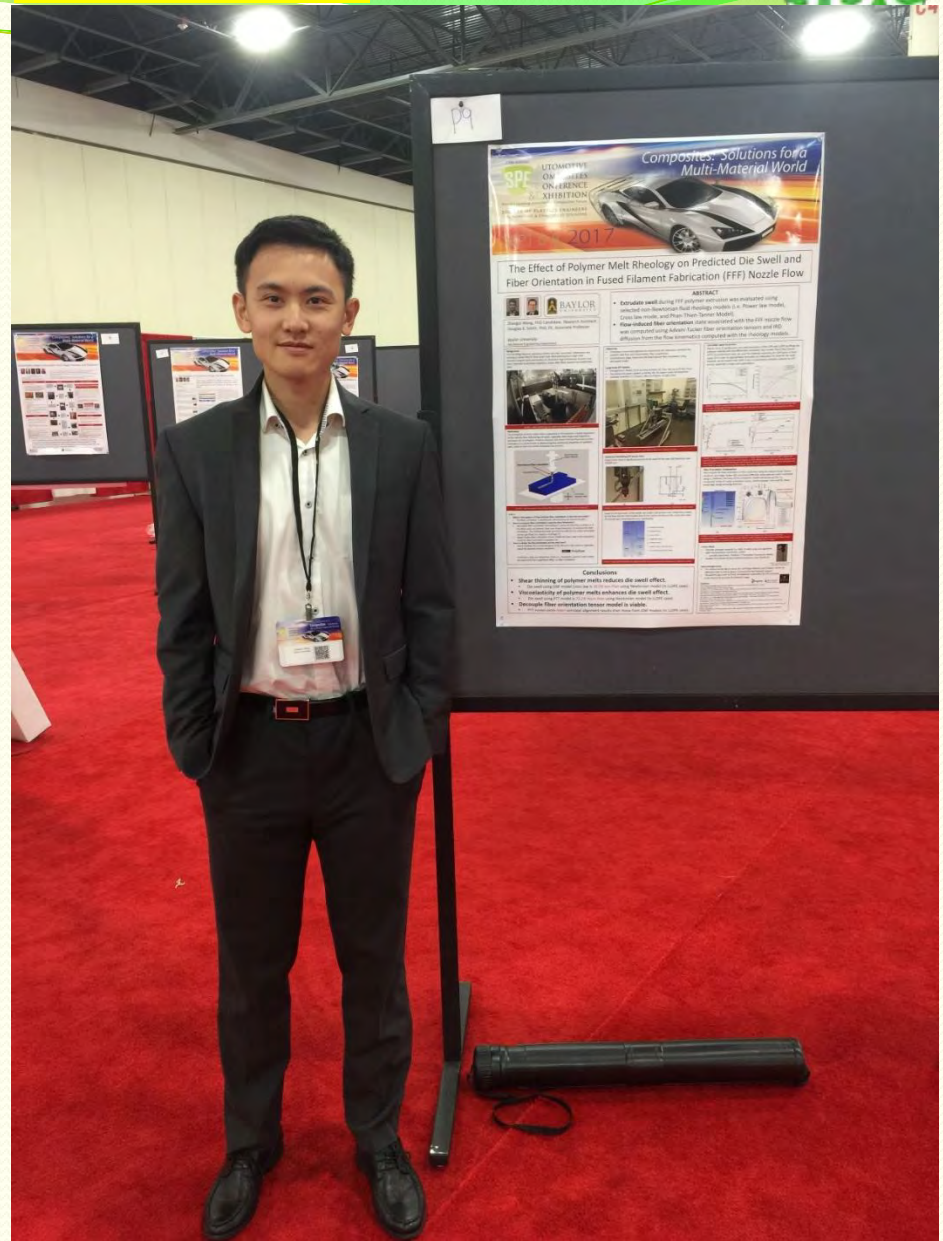
#### Acknowledgements

The authors would like to thank the Oak Ridge National Lab (ORNL) for financial support. 40004513131 as well as Baylor University for financial support.

The authors also want to thank Stratagress for corporation for the donation of the Model 20 extruder for research usage.

#### Citations

- [1] ORNL, "Large Scale FFF Printing System," Oak Ridge National Laboratory, 2017.
- [2] Z. Wang, D. E. Smith, and P. Thien-Tanner, "The Effect of Polymer Melt Rheology on Predicted Die Swell and Fiber Orientation in Fused Filament Fabrication (FFF) Nozzle Flow," *ACCE Poster*, 2017.
- [3] ANSYS, "ANSYS Polyflow," ANSYS Inc., 2017.
- [4] Stratagress, "Stratagress Model 3D printing extruder," Stratagress Inc., 2017.
- [5] G. Gargy, A. S. Gargy, and A. S. Gargy, "Die Swell Simulation of the LLDE and LLDE by Fitting the Polymer Melt Flow with the Carreau-Yasuda Flow Model," *ACCE Poster*, 2017.
- [6] F. Fowkes and J. Young, "Fiber Orientation Diffusion," *Journal of Polymer Science: Part B: Polymer Physics*, vol. 1, pp. 1-10, 1963.
- [7] D. E. Smith, "Fiber Orientation Tensor Model," *Journal of Polymer Science: Part B: Polymer Physics*, vol. 1, pp. 1-10, 2017.
- [8] D. E. Smith, "Fiber Orientation Tensor Model," *Journal of Polymer Science: Part B: Polymer Physics*, vol. 1, pp. 1-10, 2017.







SEP 16-8 2017

## Prediction of the fiber orientation state and resulting effective longitudinal modulus and CTE within large volume, 3D printed, carbon fiber filled ABS



Timothy D. Russell, Dr. David A. Jack  
Baylor University, Department of  
Mechanical Engineering

3D printing is an additive manufacturing technique that has been growing in popularity. Recent developments include large volume fused filament fabrication (FFF), a type of 3D printing, such as that done by Oak Ridge National Laboratory (Oak Ridge, TN). The large volume 3D printing machines, called big Area Additive Manufacturing (BAAM) machines, can fabricate parts on the order of several feet. In order to increase the structural capability of these large parts, discrete short fibers can be mixed into the polymer build material in order to create short fiber reinforced composite parts. Modeling the fiber orientation state within the composite extrusion is an important step in determining the material properties of the final part, such as the stiffness and coefficient of thermal expansion (CTE), which are functions of the fiber orientation state.



FIG. 1. Baylor 1D BAAM Extrusion System

The goal of this study is to compare the orientation state prediction of several fiber orientation models. Once the computational steps have been taken for several fiber orientation models, the models are compared by how well their predictions of the effective longitudinal Young's modulus  $E_{xx}$  and effective longitudinal CTE  $\alpha_{xx}$  match experimental values.

**Computational Methodology**  
A brief overview of the computational methods used in this study is given in Fig. 3.

**Fig. 3. Computational Methodology**  
Solve for the velocity gradients of the flow in the nozzle with CONSID Multiphysics. Solve for the fiber orientation state and, subsequently, the stiffness and CTE tensors in MATLAB. Simulate a tensile test and CTE test in COMSOL given the appropriate material properties obtained in step 2 and as a post processing step, calculate  $E_{xx}$  and  $\alpha_{xx}$ .

**Orientation Tensor**  
An important preliminary step is to define how the fiber orientation state will be quantified. The tensor of orientation describes the overall fiber orientation state at a point within a short fiber composite and can be defined as:

$$\bar{A}_{ij} = \frac{1}{V} \int_V p_i p_j dV \quad (1)$$

where  $p_i$  is the probability density function defined by the equation:

$$P(\theta) \propto \theta^2 \sin \theta \quad (2)$$

where the probability  $P$  that a fiber, which is direction  $\theta$  (defined by the unit vector  $\hat{p}$ ), will be pointing between the angles  $\theta$  and  $\theta + d\theta$ , and  $\hat{p}$  and  $\hat{p} + d\hat{p}$  is given as  $P(\theta) d\theta d\hat{p}$ . The angle  $\theta$  is measured counterclockwise from the positive  $x$ -axis and the angle  $\hat{p}$  is measured from the  $x$ -axis. Properties of  $\bar{A}_{ij}$  include symmetry,  $\bar{A}_{ij} = \bar{A}_{ji}$ , and the fact that the trace always equals 1, meaning  $\bar{A}_{11} + \bar{A}_{22} + \bar{A}_{33} = 1$ . In addition,  $\bar{A}_{11}$ ,  $\bar{A}_{22}$ , and  $\bar{A}_{33}$  correspond to the amount of overall alignment in the  $x$ ,  $y$ , and  $z$  directions, respectively. Different fiber orientations are represented in Fig. 4.

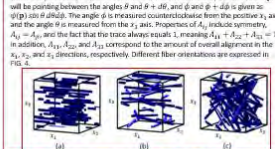


FIG. 4. Fiber orientation distributions: (a) uniaxial,  $\bar{A}_{11} = 1$ , (b) random in-plane,  $\bar{A}_{11} = \bar{A}_{22} = \frac{2}{3}$ , and (c) completely random,  $\bar{A}_{11} = \bar{A}_{22} = \bar{A}_{33} = \frac{1}{3}$

In this study, a comparison of fiber orientation models to model the fiber orientation state within a short fiber, composite, 3D printed bead is made by calculating the fiber orientation state, the subsequent spatially varying, anisotropic stiffness and CTE tensors, and the effective longitudinal stiffness  $E_{xx}$  and CTE  $\alpha_{xx}$ . Reasonableness of the models used are assessed by comparisons to experimental results for  $E_{xx}$  and  $\alpha_{xx}$ .

**Fiber Orientation Modeling**

The first step of modeling the fiber orientation state within a bead fabricated by BAAM involves defining the geometry of the large volume extrusion. This can be done in COMSOL Multiphysics as in FIG. 5, where the inlet is given an initial velocity of 7.68 mm/s, the outlet has no pressure and vertically constrained outflow, and the walls are no-slip ( $\mu = 0$ ). The geometries of the nozzle in FIG. 5 are based on the actual dimensions of a Strangegrip Extruder Model 19, which was the large volume extruder used in the experimental phase of this study. The velocity and velocity gradients were then calculated along the 70 streamlines in the flow zone in FIG. 6.

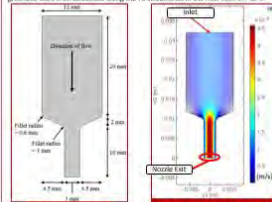


FIG. 5. Nozzle Geometry

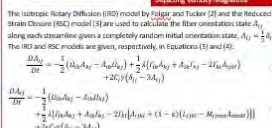


FIG. 6. Flow Solution Color Scheme

The isotropic, Rotary Diffusion (RD) model by Edgar and Taylor [2] and the Reduced Strain Closure (RSC) model [3] are used to calculate the fiber orientation state  $\bar{A}_{ij}$  along each streamline given a completely random initial orientation state,  $\bar{A}_{ij} = \frac{1}{3}\delta_{ij}$ . The RD and RSC models are given, respectively, in equations (3) and (4):

$$\frac{D\bar{A}_{ij}}{Dt} = \frac{1}{2} \left( \bar{A}_{ij} \bar{A}_{kk} - \bar{A}_{kk} \bar{A}_{ij} \right) + \frac{1}{2} \left( \bar{A}_{ij} \bar{A}_{kk} + \bar{A}_{kk} \bar{A}_{ij} \right) - \frac{1}{2} \bar{A}_{kk} \bar{A}_{ij} \quad (3)$$

$$\frac{D\bar{A}_{ij}}{Dt} = \frac{1}{2} \left( \bar{A}_{ij} \bar{A}_{kk} - \bar{A}_{kk} \bar{A}_{ij} \right) + \frac{1}{2} \left( \bar{A}_{ij} \bar{A}_{kk} + \bar{A}_{kk} \bar{A}_{ij} \right) - \frac{1}{2} \bar{A}_{kk} \bar{A}_{ij} \quad (4)$$

In equations (3) and (4),  $\bar{A}_{kk}$  is the vorticity tensor,  $\bar{A}_{kk}$  is the rate of deformation tensor,  $\bar{A}_{kk} = \frac{1}{2} \left( \bar{A}_{ij} \bar{A}_{ji} + \bar{A}_{ji} \bar{A}_{ij} \right)$  where  $\bar{A}_{ij}$  is the equivalent ellipsoidal aspect ratio,  $\bar{A}_{kk}$  is approximated in terms of  $\bar{A}_{ij}$  with the assumption,  $\bar{A}_{ij}$  is a fiber interaction term, and  $\bar{A}_{kk}$  is a strain-reduction factor to slow down the rate of alignment.

**Stiffness and CTE Predictions**  
With the newly found orientation tensor, the fourth-order, anisotropic stiffness and second-order, anisotropic CTE are found by first determining the fourth-order, transversely isotropic stiffness tensor as the Reuss-Woignot-microscopic model [4] (which uses the elastic modulus and Poisson's ratio of the fiber and the fiber aspect ratio of the fiber and the fiber volume fraction) and then using an orientation average procedure of the transversely isotropic stiffness. The fourth-order stiffness is given by:

$$E_{ijkl} = \bar{A}_{ij} \bar{A}_{kl} E_{1111} + \bar{A}_{ij} \bar{A}_{kl} E_{1122} + \bar{A}_{ij} \bar{A}_{kl} E_{1133} + \bar{A}_{ij} \bar{A}_{kl} E_{2222} + \bar{A}_{ij} \bar{A}_{kl} E_{2233} + \bar{A}_{ij} \bar{A}_{kl} E_{3333} \quad (5)$$

and the second order CTE is given by:

$$\alpha_{ij} = \bar{A}_{ij} \alpha_{11} + \bar{A}_{ij} \alpha_{22} + \bar{A}_{ij} \alpha_{33} \quad (6)$$

where  $\alpha_{11}$ ,  $\alpha_{22}$ , and  $\alpha_{33}$  are the functions of the components of the transversely isotropic stiffness and the  $\bar{A}_{ij}$ 's are functions of the components of both the transversely isotropic stiffness and CTE. Taking the anisotropic stiffness and CTE at the end of each streamline is equivalent to getting the anisotropic stiffness and CTE at the nozzle exit. Components of the fourth-order anisotropic stiffness and CTE are gradient at the nozzle exit as a function of  $\bar{A}_{ij}$  for the RSC model with varying

strain reduction factor in FIG. 7 and FIG. 8.

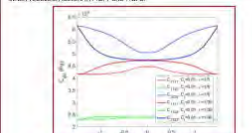


FIG. 7. Components of  $C_{ijkl}$  as a function of  $\bar{A}_{ij}$  at the Nozzle Exit

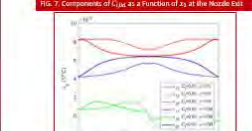


FIG. 8. Components of  $\alpha_{ij}$  as a function of  $\bar{A}_{ij}$  at the Nozzle Exit

The  $E_{xx}$  properties at the nozzle exit can be used to define the stiffness properties of a tensile test in COMSOL, on which a tensile test simulation is done to get  $E_{xx}$ . Similarly, a TMA test is simulated as a TMA sample with the  $\alpha_{xx}$  and  $\alpha_{yy}$  properties at the nozzle exit as the material properties and  $\alpha_{xx}$  is desired.

**Physical Testing**

Sample 1A fiber tests of 124 carbon fiber filled ABS from PolyChix fabricated by Baylor's large volume Strangegrip Extruder Model 19 shown in FIG. 1, were used for physical tensile testing and TMA testing. Thirty-three tensile tests at a constant rate of 5 mm/min were performed with a Test Resources tensile machine with a 5 kip load frame and an optical extensometer. Nine TMA tests with ramps -40°C to 120°C at 2°C/min were tested with a TA Instruments TMA Q400. The average experimental value of  $E_{xx}$  was 3.55 GPa with a standard deviation of 0.27 GPa. The average experimental  $\alpha_{xx}$  was  $5.69 \times 10^{-6}$  (1/°C) with a standard deviation of  $1.27 \times 10^{-6}$  (1/°C). A comparison of the RD and RSC models with varying strain-reduction factors and the average experimental values is summarized in Table 1, where the absolute percent relative error was calculated with the following formula:

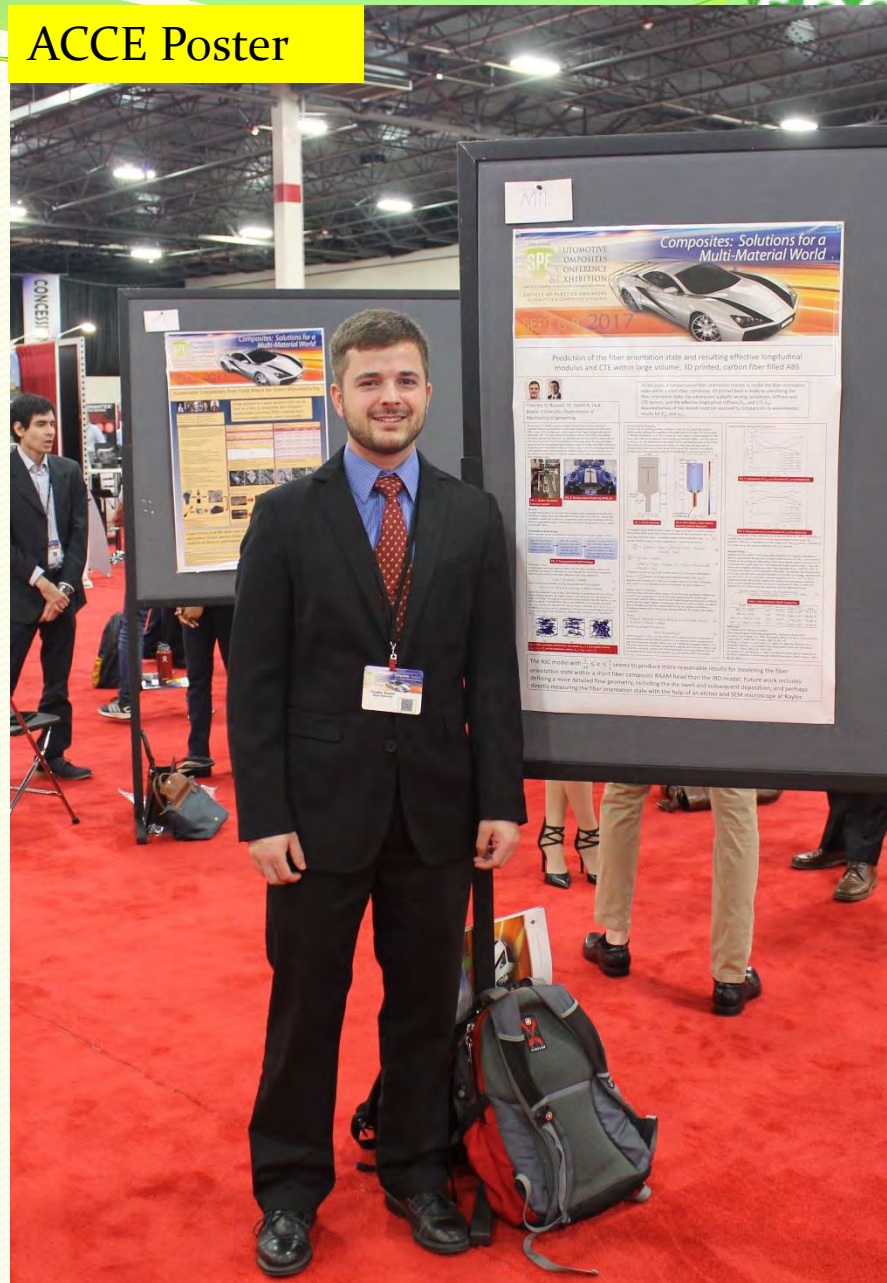
$$E = \frac{|\text{Model value} - \text{Average experimental value}|}{\text{Average experimental value}} \times 100\% \quad (7)$$

Table 1. Fiber Orientation Model Comparison

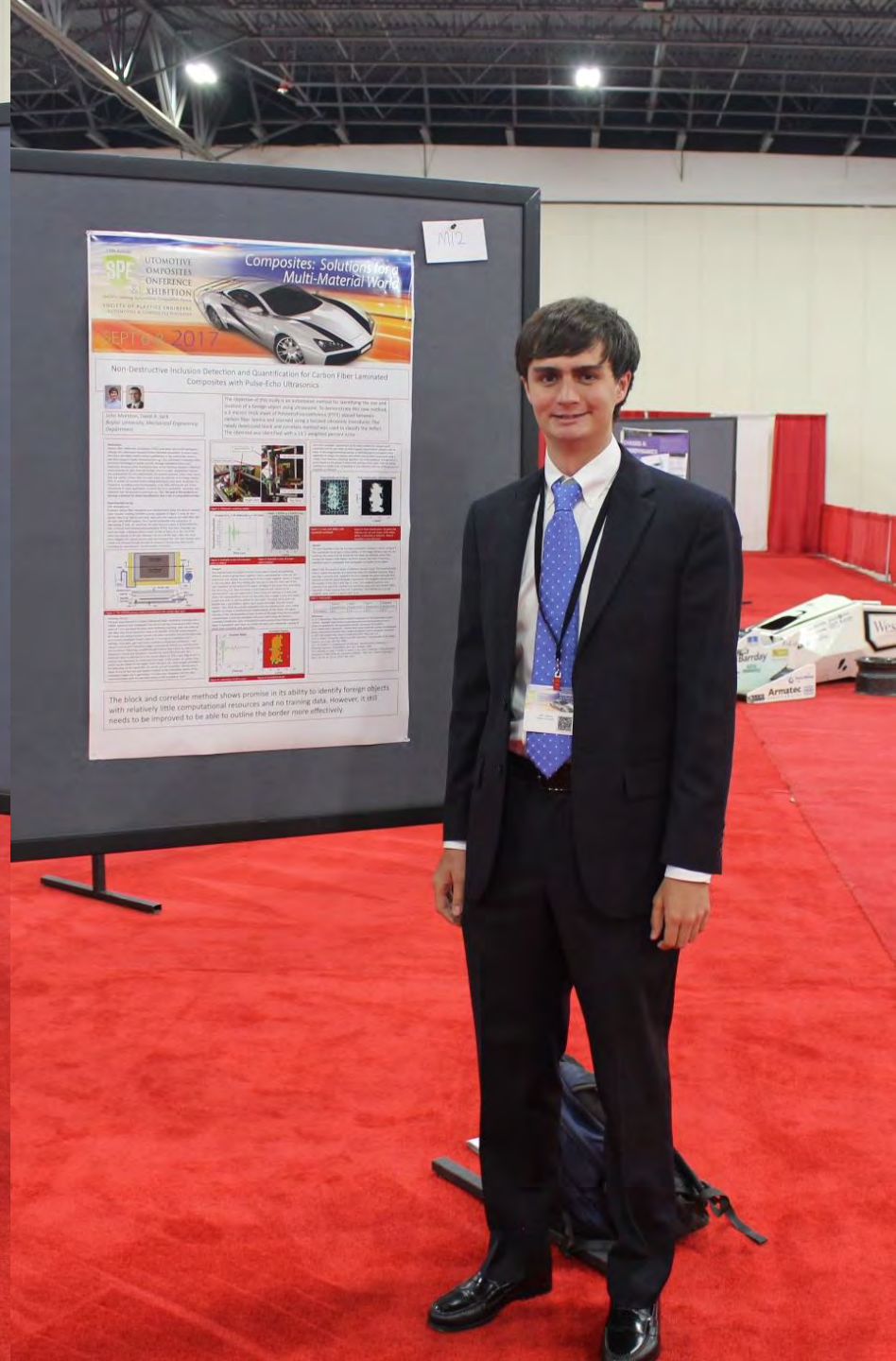
Model Used	$E_{xx}$ (GPa)	$\alpha_{xx}$ (1/°C)	$E_{xx}$ Error (%)	$\alpha_{xx}$ Error (%)
RD, $C_2 = 0.001$	4.85	36.4%	$9.62 \times 10^4$	81.11 %
RD, $C_2 = 0.01$	4.42	24.1%	$2.00 \times 10^4$	60.62 %
RSC, $C_2 = 0.01$ , $\kappa = 1/5$	3.90	9.90 %	$3.78 \times 10^3$	23.46 %
RSC, $C_2 = 0.01$ , $\kappa = 1/10$	3.37	5.10 %	$5.93 \times 10^3$	16.46 %

**References:**  
[1] "Shelby" (Online). Available: <http://web.org.gov/online/shelby/>. [Accessed: 28 Aug 2017].  
[2] Edgar, F., and Taylor, C. L., 1984, "Orientation Behavior of Fibers in Concentrated Suspensions," *J. Appl. Polym. Sci.*, **19**, pp. 19-39.  
[3] Wang, A., O'Gara, J., and Nader, C., 2008, "An Objective Model for Flow Orientation Behavior in Concentrated Fiber Suspensions: Theory and Mechanical Evidence," *J. Rheol.*, **52**(5), pp. 1197-1205.  
[4] Onogi, S. P., and Wang, J. L., 1984, "The Effect of Aspect Ratio of Inclusions on the Elastic Properties of Discontinuously Aligned Composites," *J. Appl. Polym. Sci.*, **37**, pp. 327-333.

## ACCE Poster









SEPT 6-8, 2017

# Composites: Solutions for a Multi-Material World



## Implementation of LVDT to Decrease Time Associated with Ultrasonic Scans of Carbon Fiber Composites



Nathaniel Blackman, M.S. (expected 2019)  
Dr. David Jack (advisor)  
Baylor University, Mechanical Engineering

**ABSTRACT:** Using a LVDT to track linear positioning, scan times associated with traditional C-scanning techniques can be dramatically reduced.

### Objective

The current c-scanning techniques used to further research in the non-destructive testing (NDT) of carbon fiber composites often require large amounts of time, slowing the ability of researchers to make significant progress. Scan times used to find small defects and inclusions over a large area, or to identify the ply orientation of complex weaves can take a prohibitively long time. This high time cost can make large and high precision NDT scans prohibitive, and makes the furthering of research difficult. Such time costs also make these advanced applications with ultrasonic scanning less appealing to those in industry. An example of the process used in NDT research can be seen in Figure 1.

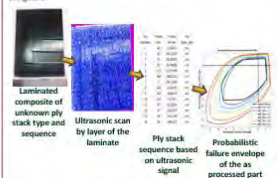


Figure 1: Example of Ultrasonic NDT

Formerly, in order to ensure that a scan was taken at the correct point, the motor would stop at each individual location to be scanned. A goal was set to allow the motor to move continuously through all locations to be included in a b-scan, and correctly scan when the ultrasonic transducer passed over each location to be included in the scan.

### Methodology

1. The ultrasonic c-scan system, did not initially have any methods installed that allowed the motor to move while tracking their position. First a rotary encoder was installed on the XZ axis to track positioning.



Figure 2: Scanning setup



Figure 3: Rotary encoder initially used to track position

2. After installing the rotary encoder, the software used for c-scanning was changed to read the digital outputs of the encoder. After testing, it was found that noise and the encoder's resolution created significant problems with use of the encoder.

3. While a decrease in the time of scans was achieved, the encoder was found to be unpredictable.
4. A linear variable differential transformer, LVDT, was installed on the XZ axis to track positioning.



Figure 4: Spring-assisted LVDT mounted to XZ axis

5. The LVDT was calibrated, and using a linear regression in MATLAB a relationship was established between changes in voltage and steps taken by the motor.
6. The software was changed to read the voltage output of the LVDT and fire when the voltage change corresponded to the desired change in steps.
7. Results of the scans were compared to those of scans taken with the old point by point logic.
8. Data was taken to identify the max speed the XZ motor can be operated while accurately tracking positioning.
9. Using the knowledge gained, a LVDT was installed on a portable scanner; see Figure 7, to increase scans of composites that need to be scanned without using an immersion setup.

### Results

1. Several successful c scans have been taken using the LVDT and continuous scanning method, and data from continuous scans and scans taken with the old software have been compared to determine the continuous scanning works. Figures 5 and 6 compare a b-scan at the same location for each scanning method, and Figures 7 and 8 compare a c-scan image the same depth into the part.

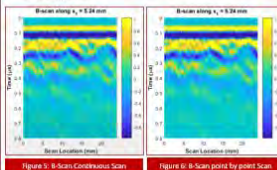


Figure 5: B-scan Continuous Scan

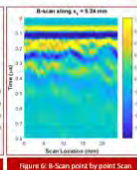


Figure 6: B-scan point by point Scan

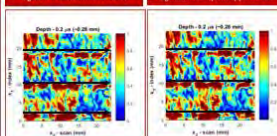


Figure 7: C-scan Continuous Scan

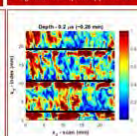


Figure 8: C-scan point by point scan

2. Using the current LABVIEW software, the motor being tracked by the LVDT can be run at speeds up to 48 times greater than the step size per increment for the motor.
3. As shown in Table 1, the scanning software takes 20% of the scan time for the standard scan used to determine ply detection of carbon fiber composites. The new scanning method has been found to take as little as 10% of the time of highly extensive scans when run at max speed.

Table 1: Standard Ply Detection Scan Times

	Point-by-Point Scan	Continuous Scan
Time to Scan	6300.4 seconds	1264.32 seconds

### Acknowledgements

I would like to thank my advisor Dr. Jack for his guidance and help. I would also like to thank Mr. Ben Wandford for his help in installing and calibrating the LVDT. Finally, I would like to thank L3 Communications and Baylor University for their support.

## ACCE Poster



By using a LVDT to track the motion of the ultrasonic transducer during a c-scan, an accurate and fast c-scanning method was developed. This method of scanning consistently saves 80% to 90% of the time required using older scanning techniques, and is being used to further ultrasonic NDT research on carbon fiber composites.



SEPT 6-8, 2017

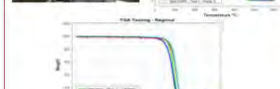
## Finite Element Analysis and Material Characterization of Structural Railroad Ties with Recycled Composites



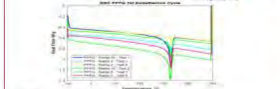
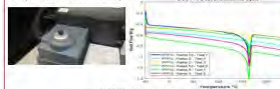
**Daniel Paul Pulipati**  
Advisor: Dr. David A. Jack  
Sponsor: AXION STRUCTURAL INNOVATIONS  
Baylor University, Mechanical Engineering

The largest volume of material within the final processed structural member is recycled high density poly ethylene (HDPE) that is obtained from a variety of vendors/manufacturers. The second largest material by volume used in the fabricated product is a recycled polypropylene/ fiberglass system that comes from a post industrial process typically associated with the automotive industry. Several tests are done using the HDPE, PP/FG and Regnet samples and some results are presented.

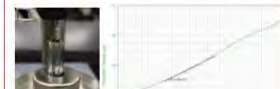
**Material Characterization**  
TGA (Thermogravimetric analysis)  
TGA is often used to identify the thermal degradation temperatures and can be helpful in capturing appropriate blend ratios.



**DSC (Differential Scanning Calorimetry)**  
Differential Scanning Calorimetry measures the amount of energy placed into a sample or extracted from a sample.



**TMA (Thermomechanical Analysis)**  
The thermomechanical analyzer (TMA) is often selected as the device of choice for characterizing the coefficient of thermal expansion (CTE) for polymers and polymeric systems.



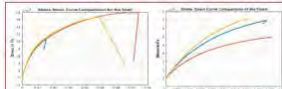
**Tensile Testing**  
Tensile testing is used to predict how a material will react under types of forces. Many material properties can be calculated, such as Young's modulus, ultimate strength, fracture point, and so on. Young's modulus is one of the key properties that is included in the finite element model analysis.

Using Micromechanics models and experimental testing, the deformation of the composite tie and the material properties are estimated to be well within experimental error. Material Characterization testing baseline aids the quality control of the plastics used in the manufacturing process and reduces the internal rejection ratio of the tie.

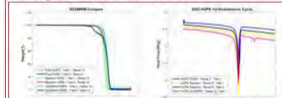


The purpose of this research is to improve the quality control test procedures and the final part performance of railroad ties, structural mats, knuges and other applications fabricated from recycled post-consumer/post-industrial waste composed of HDPE (high density poly ethylene) and PP/FG (Poly Propylene/Fiber Glass) both within the manufacturing process and the recycled materials. A technical challenge in producing the final part performance is a limited understanding of the mechanisms contributing to the spatially varying material properties. In addition, there is potential variability

by collecting various material samples and performing tests to identify potential areas of variability, i.e., calorimetry, thermal decay, moisture content, moldability, rheological testing, and structural testing of tensile (specimen) characterization of the materials can be achieved, which will also aid in the process of quality control. Select characterization results are presented within this poster to highlight the early results in this study. A Finite Element Analysis (FEA) is also presented that incorporates testing of the composite railroad ties to aid in establishing the optimum testing protocol. The FEA model allows the study of different loading mechanisms and predicts the structural response of the ties.



Notable differences with material characterization



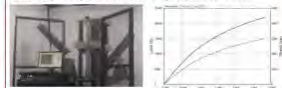
### Composite railroad tie

A typical composite railroad tie has a dimension of 72"x12"x8". The cross section of a railroad tie is shown below with the core and shell regions. The shell region is the outer layer of the tie which is fully solid, and a bonded core inner region, which has air gaps (voids). The core region is significantly weaker than the shell region. Current research focuses on shell, core regions and micro-mechanics modeling.



### Four Point Bend Test

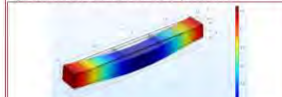
The figure below shows a typical test report from a four point bend test. The graph shows the load (lb) vs position (in) relationship and the failure occurs approximately at 23000 (lb) force with about 2.86 inches of displacement on the left y-axis. The x-axis on the right side shows the values of stress (psi) as a function of position (in). At 10000 lbs., the displacement is 0.748 inches.



### Finite Element Analysis (FEA)

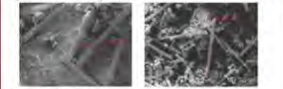
Assumptions for the finite element modeling:

- The tie is isotropic.
- A step change is assumed at the interface between the shell and the core region.
- The tie is linear elastic in deformation to the loading conditions.
- Geometry is measured from a manufactured tie and the fillets are approximated along the edges.
- The initial modulus of elasticity (material property) results are taken from tensile testing (Note: this is only for the first set of results).
- Material properties are obtained from micromechanics models based on the constituent properties of the fiber and the matrix (Note: this is the case for all cases, except the first).
- Shell wall thickness is constant at 3/4" of an inch.
- The finite element model of the tie is designed with a shell and core region as seen in the railroad tie. The displacement obtained from FEA is 0.755 inches, compared to the 0.748 inches experimentally which is less than 1% error. The figure below shows the displacement in the Z component in meters.



### Aspect Ratio

To calculate the aspect ratio, a few sections of the tie were taken and burned in a furnace until only tags and glass fibers are left. The glass fibers are then put on double sided copper tapes, placed on an aluminum target, and placed within our JEOL JSM Scanning Electron Microscope. The lengths and diameters are measured at 200x and 500x magnification and select images are shown. The aspect ratio was statistically calculated to be 25.



### Micro-Mechanics Modeling

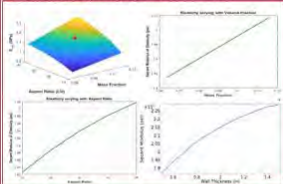
- Procedure for approaching the Micro-Mechanics Model:
- Determine the Aspect Ratio.
- Determine the material properties.
- Predict Toffness matrix and Young's modulus from fiber orientation models.
- Use the obtained Young's modulus as input to the COMSOL model and performing different characteristic studies.

The modeling of composite properties is done using the Tachian Wang model as fully expressed by a previous Baylor graduate student (Cong Zhang, M.S. 2011). The inputs to this model are Young's modulus, Poisson's ratio, Coefficient of thermal expansion of the matrix and the fibers, aspect ratio and volume fraction. The matrix here being a mixture of HDPE and PP. Aspect Ratio in this case is defined as the ratio of the length of the fiber to the diameter of the fiber. This information is vital to Micro-Mechanics modeling as the aspect ratio of the fiber is a key variable and as the aspect ratio increases many of the bulk material properties also increase. The tensile modulus of 1.13 GPa is calculated, which is comparable to the 1.14 GPa GPa obtained experimentally.

Parameter	Constituent Values from Data
Modulus of Matrix	800MPa
Modulus of Fibers	80GPa
CTE of Matrix	120E-6 / °C
CTE of Fibers	4.5E-6 / °C
Poisson's ratio of Matrix	0.45
Poisson's ratio of Fiber	0.23
Aspect Ratio	25
Volume Fraction	0.035

### Parametric Studies

The parameters changeable without changing the matrix or fiber properties is the volume fraction of glass fiber, aspect ratio and wall thickness.



### Conclusions

- Material characterization testing is useful to know the range of characteristics of the material trends that are most efficient for production.
- For HDPE, TGA testing clearly suggests the general trend of decomposition.
- Quality control in turn helps with the reduced failure rate in production.
- Finite element analysis is comparable to the experimental four point bend testing and the material properties from tensile testing and Micro-mechanics modeling is comparable.
- Parametric studies help predict the output modulus with changing aspect ratio, Mass fraction and wall thickness.

## ACCE Poster







# Composites: Solutions for a Multi-Material World

SEPT 6-8, 2017

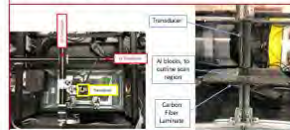
## Determining Ply Orientation for Unidirectional Carbon Fiber Laminated Composites Utilizing an Ultrasonic Technique



Author: Benjamin Blandford  
Advisor: Dr. David A. Jack  
Sponsor: L3 Technologies  
Baylor University, Mechanical Engineering

Carbon fiber composites are used extensively in the automotive industry, and have found popular use in the aerospace and athletic industries. However, due to the nature of carbon fiber manufacturing it is often not economical, and sometimes incorrect to use traditional destructive testing techniques. Destructive techniques are costly as they often ruin the final component. To aid in the desire to prevent the destruction of the composite component being investigated, non-destructive testing techniques may be employed. This research uses a custom pulse-echo ultrasonic transducer and immersion system to scan and collect data from in-house fabricated unidirectional carbon fiber laminated composites. The unidirectional fabric used in this research contains a small weft fiber that runs perpendicular to the carbon fibers. The weft fiber makes fabrication easier, and does not provide structural support. Scanning and data collection is performed with an in house Labview code and data is post processed with a custom MATLAB code. Ply orientation is determined based off detecting the weft fibers using the peak signal information within a selected gate in the associated C-scan and recognizing that the weft fiber and carbon fiber are perpendicular to one another. Results presented show that ply orientation can be accurately predicted for the investigated unidirectional carbon fiber composites that incorporate a weft fiber perpendicular to the carbon fibers.

**Scanning set up:**  
A Ultrasonic pulser/receiver is used in a pulse/echo configuration with a sampling rate of 100MHz. Various transducers are used in this research and include a 10MHz, 100kHz, 150kHz, and a 250kHz. A Winbox translation system is used to traverse the ultrasonic transducer. The scanning (XZ) direction uses a custom threaded screw (200 displacement) and the rotary (YZ) direction uses a four screw (300 displacement). Labview is used to translate the transducer and capture the scan data.



Part B places inside a water tank on a custom built, adjustable, leveling stand. This assumes the scan region is in focus with the transducer.

**Composite Fabrication:**  
Uni-directional composites are fabricated in house using fiber, carbon fiber from Soltec Composites with Proseal IN-114 resin and Proseal IN-221 hardener. A wet layup technique is used for fabrication. After the laminates are stacked on the aluminum tooling - with a generous amount of resin - vacuum bagging is secured around the part and vacuum is pulled to remove the excess resin. The parts are cured in a furnace for 12 hours. This specific uni-directional carbon fiber contains a weft fiber. The weft fiber does not provide any mechanical improvements to the carbon fiber. The weft fiber is there to hold the individual carbon fibers in place to allow for easier manufacturing. A total of (2) uni-directional parts were fabricated for this study. Both parts had 9 layers and they had identical orientation. The only difference is one was manufactured with the weft fiber facing the sock side of the fabrication plate and the other part was fabricated with the weft fiber facing the bag side. Below are images of both parts. The scanning for each part is as follows: (in degrees off of XZ) 0-30-45-60-90-60-45-30-0.

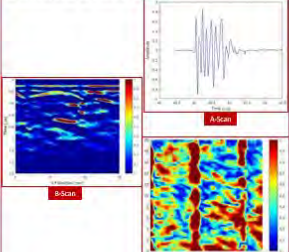


The composite on the left (Part A) was fabricated with the weft fiber against the tool. The composite on the right (B) was fabricated with the weft fiber against the bagging.

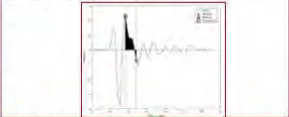


Two scan points not the weft fiber and the carbon fiber angle  $\theta_y$ .

**Scanning Procedure:**  
In house Labview code with Distance Amplitude Correction is used to control various stepper motors, and fire the ultrasonic transducer. Our software is a continuous scanning system that does not have to stop to collect an A-scan (the system moves continuously in the scanning direction until the user defined limit is reached). A-scans are collected over the entire scan region. The research used scanning regions ranging from 10mm X 10mm to 200mm X 200mm. The A-scans are compiled to form a B-scan, which shows the cross section of the carbon fiber composite while we move in a specific direction. The XZ cross section as you move through XZ. C-scans are also developed and show the planar surface as you move through the part (through time). A sample A-scan, B-scan, and C-scan are shown below.

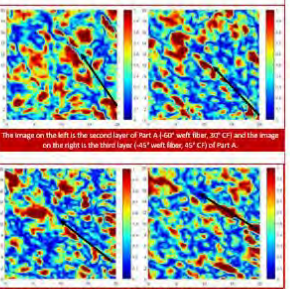


**Analysis Techniques**  
When carbon fiber composites have very small height difference due to the nature of a weft fiber. These height differences allow for visual interpretation of C-scans to determine ply orientation. Because uni-directional carbon fiber composites are flatter in plane, another technique must be used. The weft fiber runs perpendicular to the carbon fibers. There is a height difference between the weft fiber and carbon fiber as well as a material difference. Detecting the weft fiber allows us to determine ply orientation. Below is an A-scan that shows the analysis techniques.



Four analysis techniques are used: maximum value, minimum value, absolute maximum value, and an absolute value integral average. The integral average is the sum of the absolute value within the shaded project divided by the distance between the two vertical dotted lines. This distance is the length of the gate, which is a time.

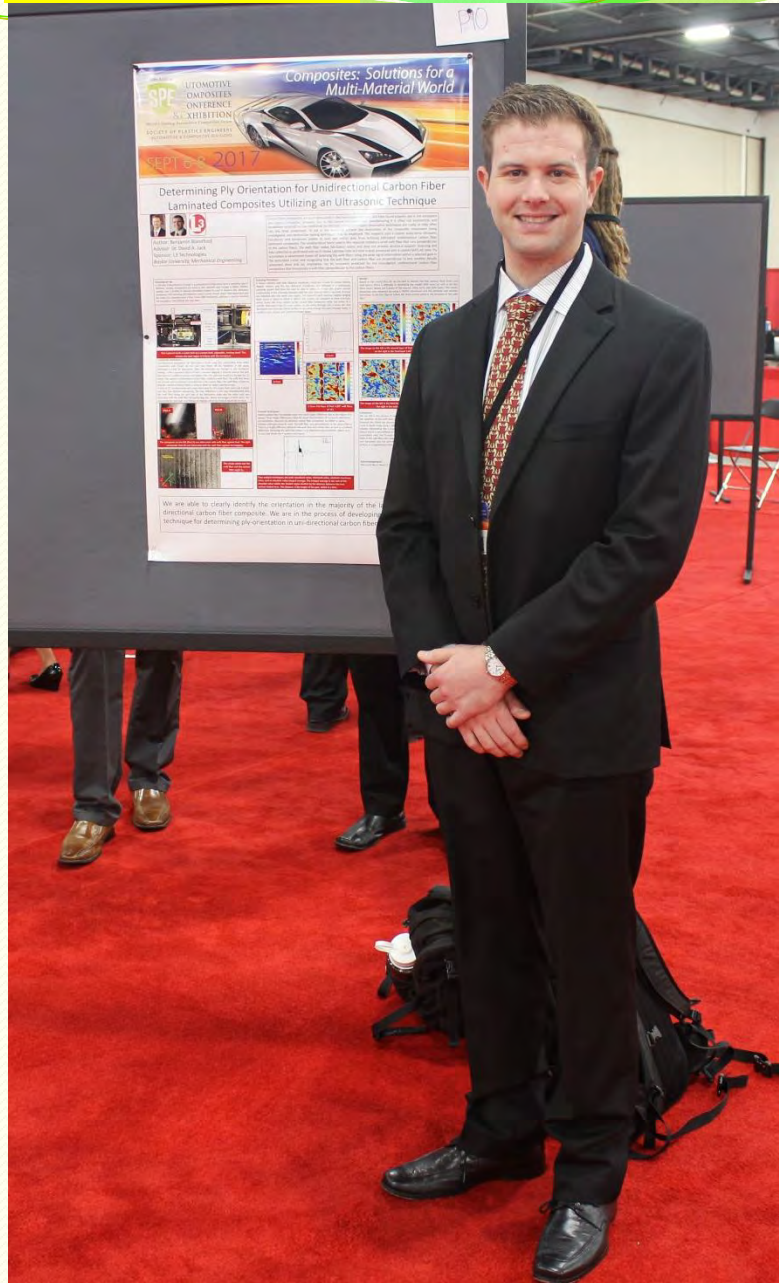
**Results**  
Based on the results thus far we are able to identify the first, second, third, fourth, and sixth layers. There is difficulty in identifying the middle (fifth layer) as well as the last three layers. Below are C-scans of the second, third, fourth, and sixth layers. The results presented were obtained by using a 150kHz transducer and the absolute max analysis technique. In the four figures below, the black arrow point in the direction of the weft fiber.



**Conclusion**  
We are still in the process of modifying the MATLAB code to more precisely determine the direction of the weft fiber. Only the 150kHz transducer results are presented here, however the 150kHz has proven to be produce decent results. The next step includes a more in depth study using a 250kHz transducer. The long term goal is to move away from visually interpreting the C-scan data to obtain the ply-orientation. Results have also shown that it is very difficult to detect repeat layers, that are not separated by a different orientation. Also, Part B tends to have small voids on the surface of the part, on either side of the weft fiber; this makes it difficult to get good scans. Part A, the composite that was fabricated with the weft fiber against the bag, not only provides a much smoother surface, it is hypothesized that it yields much clearer results.

**Acknowledgements**  
We would like to thank L3 Technologies for their continual support.

## ACCE Poster





# The Applicability of Simplified Viscoelastic Fluid Model to Predict Extrudate Swell and Fiber Orientation in Fused Filament Fabrication Nozzle Flow

Zhaogui Wang

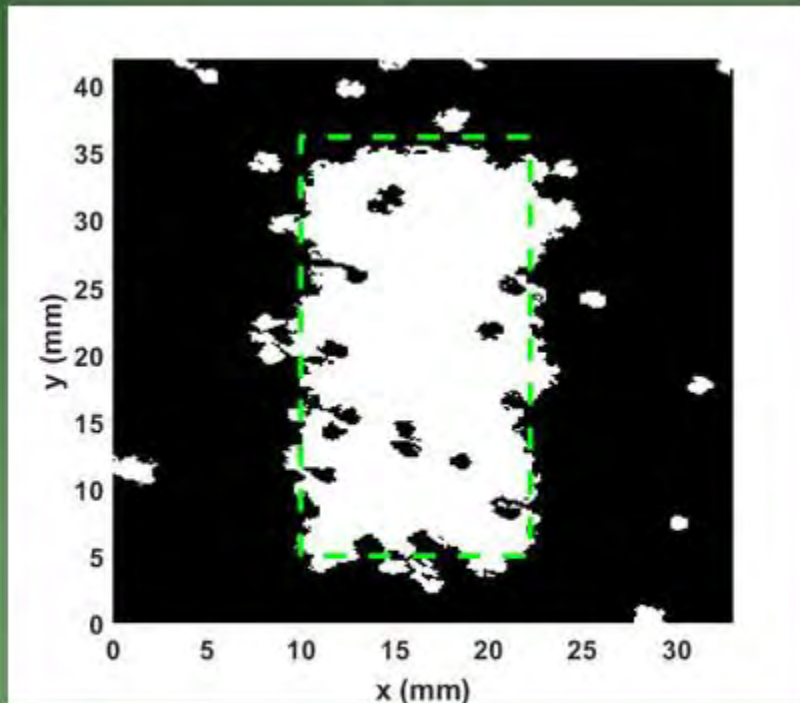
PhD Candidate, Research Assistant  
Mechanical Engineering, Baylor University  
[Zhaogui\\_Wang@baylor.edu](mailto:Zhaogui_Wang@baylor.edu)

Douglas E. Smith, PhD, PE

Associate Professor, Graduate Program Director  
Mechanical Engineering, Baylor University  
[Douglas\\_E\\_Smith@baylor.edu](mailto:Douglas_E_Smith@baylor.edu)



# Non-Destructive Inclusion Detection and Quantification For Carbon Fiber Laminated Composites with Pulse Echo Ultrasonics



John Moreton, Master's Candidate

David A. Jack, Associate Professor

Given at the 2017 SPE ACCE Meeting,  
September 6, 2017





BAYLOR  
UNIVERSITY

# Conference Attendance – Polyolefins



- We attended our Polyolefins conference 2018 in Houston, Texas.
- We had 5 students attend and help with the conference.









## EXPERIMENT ON MECHANICAL PROPERTIES OF CHOPPED NATURAL FIBER REINFORCED COMPOSITE MATERIALS

**Jingtao Shuang**  
**Advisor: Dr. William Jordan**  
*Department of Mechanical Engineering*  
*Baylor University, Waco, TX*

### Experimental Process – Fiber preparation

- banana fibers were stored in a humidity-controlled environment for twenty-four hours to ensure consistent moisture content for all fibers
- These fibers were then dried out in an oven at 60°, a temperature well below the decomposition temperature, for two hours
- A volume fraction of 10% was chosen for the fibers similar to previous experiment results



### ABSTRACT:

Banana pseudo-stem fibers have potentials for applications requiring a high strength-to-weight ratio, and bear advantages of sustainability and low cost. However, the hydrophilic nature of the fibers and the hydrophobic nature of the polymer result in poor bonding between them and less composite properties. PLA is also among one of those most widely used biodegradable polymers, in various applications such as biomedical applications, bottle production, and compostable food packaging. This research investigates the mechanical properties of banana fiber reinforced PLA (Polylactic acid). It has been observed that ultimate tensile strength and Young's modulus of reinforced PLA increase with comparison to non-reinforced PLA.

### Experimental Process – Stress-strain Test

- tensile bars were tested to failure using the Test Resources DG.1000 Actuator under a 4.4 kN load cell
- The rate of 25 mm/min was chosen to run all these tests

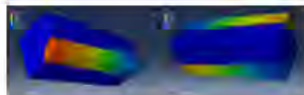


### RESULTS – Ultimate Tensile Strength and Young's modulus



### Experiment Summarization:

Material	Tensile Strength (MPa)	Young's Modulus (GPa)	Mass Density (g/cm³)
PLA	40.2	2.67	1.25
PLA + Banana Fiber	54.2	3.30	1.25



### Experimental Process – Samples from Mixer and Injection Molding

- The Braebender mixer was used to obtain the composite mixture of PLA and banana fiber at 180°C
- the resulting mixture composite of PLA and banana fibers from the Braebender mixer was cut into small pieces
- Tensile bars (Type 1, "dog bone") conforming to the ASTM D883-14 for tensile properties of plastics were then made using the DSM Xplore micro 12cc injection moulding machine
- The melt temperature and barrel temperature were set at 180°C for the composite PLA and at 190°C for the PLA only



### CONCLUSIONS

- Banana fiber reinforced PLA had a higher ultimate tensile strength when compared to clean PLA
- Reinforced PLA had an ultimate strength of 54.2 MPa whereas clean PLA had an ultimate strength of 40.2 MPa
- Overall composite polymer had a median Young's modulus of 3.30 GPa, while clean PLA had a median of Young's modulus of 2.67 GPa
- PLA and banana fibers composite is a stronger material than raw material alone

### FUTURE WORK

- Finite element method is capable of evaluating the mechanical properties of chopped natural fiber reinforced composite
- Various parameters, such as dimensions, geometries, aspect ratios, volume fraction, and interfaces, could be modeled effectively
- Python subprograms could be utilized to obtain further results of mechanical properties of composite material from the original data from Abaqus results
- To carry out numerical simulation with FEM program of chopped natural fiber reinforced thermoplastic composite materials
- To test the feasibility of numerical method through a comparison of experimental results of injection moulded parts
- To take into consideration of fiber orientations and fiber flexibility as well

### ACKNOWLEDGMENTS

I would like to thank Baylor University for its financial support. In addition, I would like to thank my advisor Dr. William Jordan for his guidance.

### REFERENCES

- [1] Venkateshwaran, N., and A. Elaiyaperumal. "Banana Fiber Reinforced Polymer Composites - A Review." *Journal of Reinforced Plastics and Composites* 29, no. 15 (2010): 2387-96.
- [2] Malkapuram, Ramakrishna, Vivek Kumar, and Yuvaraj Singh Negi. "Recent Development in Natural Fiber Reinforced Polypropylene Composites." *Journal of Reinforced Plastics and Composites* 28, no. 10 (November 20, 2006): 1169-89.



## Jingtao Shuang - Polyolefins Conference 2018 - Poster





# MICRO-MECHANICS MODELING AND MODEL VALIDATION FOR COMPOSITE RAILROAD TIES MADE FROM RECYCLED POLYOLEFINS



Daniel Pulipati, PhD Student  
David A. Jack, Associate Professor

Given at the 2018 SPE Polyolefins  
Conference, February 28, 2018.







# Conference Attendance – ANTEC



- Baylor SPE was awarded 2<sup>nd</sup> place for SPE chapter of the year at ANTEC 2018.
- 1 Podium Presentations
- 4 Poster Presentations





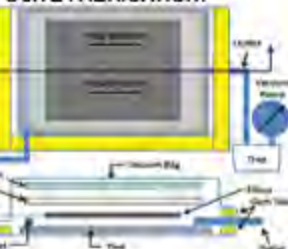
# Nondestructive Testing Technique to Inspect Internal Delamination of Carbon Fiber Polymer Matrix Laminates

**Author: Benjamin M. Blandford**  
**Advisor: Dr. David A. Jack**  
*Department of Mechanical Engineering,  
Baylor University, Waco, TX*

## INTRODUCTION:

Due to the nature of carbon fiber composite structures, damage can be present on the surface of the part without any visible signs of damage on the external surface. Damage/delamination of any sort negatively impacts the composites material properties. This study uses an ultrasonic immersion system to visually determine the extent of internal damage caused by low-velocity impacts.

## COMPOSITE FABRICATION:



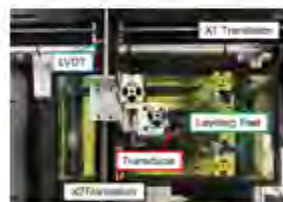
All composites are fabricated in house using a VARTM (Vacuum Assisted Resin Transfer Method) technique. A 3K/8oz plain weave carbon fiber is used with Proset INF 114 resin and Proset INF 211 hardener. Laminates (7-in x 10-in) are manufactured and then cut out to approximately (3-in x 8-in) for drop tower testing. This study looks at an 8 lamina laminate [0/45/0/45].



A tile saw is used for cutting the carbon fiber laminates. Once laminates are cut to size they are scanned using a custom ultrasonic C-scan immersion system to get the baseline undamaged results. The laminates are then subject to low-velocity impacts and surface damage is minimized. The damaged laminates are then scanned again and the results are compared to the undamaged results.

## IMMERSION C-SCAN:

In house LabView code has been used to perform ultrasonic C-Scans. For this study a 15 MHz spherically focused transducer was used in a pulse-echo configuration. Other equipment include a US 160MHz pulser/receiver, Velmex immersion stages, and an RDP LVDI. This used a scan resolution of 0.2-mm per pixel and has the capability to scan at 100mm per A-Scan. The scan area is set to 100mm x 2-in and an aluminum L is placed in the bottom left corner. This marks the location of the scan. This ensures that undamaged and damaged scans are taken over the same region. A-scans are taken along the scan path.



## ABSTRACT:

Carbon fiber reinforced polymers have a wide range of applications, from the most advanced fighter jets to golf club shafts, and everything in-between. Carbon fiber composites provide a favorable strength to weight ratio compared to traditional metallic materials used to fabricate these same components. However, additional in-situ testing techniques need to be employed to evaluate carbon fiber components, specifically in regards to determining and quantifying damage. Damage, in the form of delamination, can arise from a host of reasons as varied as a technician dropping a wrench while performing maintenance or a minor flaw in the production process. Due to the layered structure of carbon fiber composites, damage may be present in an interior lamina with no visible sign of damage on the external surface. Traditional destructive testing procedures are not acceptable as not all damage results in a failed component, and there may be a desire to keep the carbon fiber component in service in order to lower production costs. This research uses a custom drop tower to impact carbon fiber laminates in a manner as to minimize surface damage, while at the same time producing internal damage to the laminate. An in house immersion system paired with a custom LabView code is used to perform ultrasonic scans on the laminates. Data is post processed in MATLAB to determine the extent of the damage that is not visible on the surface. Current results show an ability to see internal damage even when there is minimal to no surface damage, and the zone of identified internal damage is larger than that initially anticipated.

## LOW VELOCITY IMPACT:

An in house drop tower is used to damage the carbon fiber laminate. The carbon fiber laminate is placed in the laminate holder and clamped in place. Pneumatic cylinders are used in conjunction with an Arduino controller to prevent subsequent impacts. The mass of the impactor and sled is 2.5Kg and the distance between the impactor and top surface of the laminate ranges from 0.1m to 0.15m. These values result in an impact velocity of  $1.40 \frac{m}{s}$  to  $1.72 \frac{m}{s}$ .

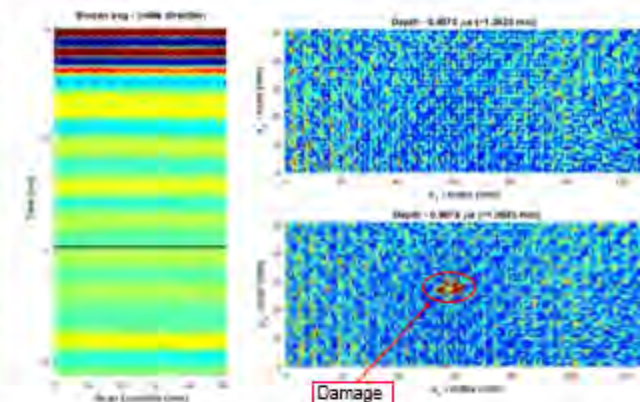
This study is interested in low velocity impacts for purposes of simulating events such as a technician dropping a wrench, or other blunt object, on to a carbon fiber component. The tip of the current impactor is flat and has a diameter of approximately 8.5mm.



## RESULTS:



The image on the left shows the damage which resulted from an impact. The impact zone is marked with a white circle. The damage is extremely difficult to see any damage. At just the correct angle and small dent is semi visible.



The images above are frames of a C-scan video. Both images are at the same depth in the laminate. The depth is shown in the B-scan on the left of the C-scan image. The top C-scan is taken prior to subjecting the laminate to impact damage. The bottom C-scan is taken after the laminate is subjected to impact damage. By comparing the two images it is seen that there has been a change in the C-scan results. This change is circled in black on the damaged C-scan image. A depth more than half way through the laminate is chosen to show that damage is seen beyond just the first couple of layers. The damage width is measured to be approximately 10mm, which is just slightly larger than the diameter of the impactor (8.5mm).

## CONCLUSIONS:

The current study shows that an immersion tank ultrasonic scanning procedure is a viable option for determining the extent of unseen damage in a carbon fiber laminate composite. Due to the current drop tower configuration, it is believed that the damage from the drop tower is tearing the laminate due to bending of the carbon fiber lamina. This is because there is nothing to support the back side of the laminate. In real world aerospace/automotive composite structures there is honeycomb structure, or other rigid structures on the back side of the carbon fiber. There is also a metallic structure or more carbon fiber on the other side of the rigid structure. This creates a sandwich structure that is much more resistant to bending. Damage scanning this type of sandwich structure is the next step for this research.



# EFFECTS OF SCREW MOTION ON PREDICTED FIBER ORIENTATION IN LARGE SCALE POLYMER COMPOSITE ADDITIVE MANUFACTURING

Zhaogui Wang  
Advisor: Douglas E. Smith

Department of Mechanical Engineering,  
Baylor University, Waco, TX

## BACKGROUND

Extrusion-based rapid prototyping has moved to fabrication of large size parts and tooling (see Fig. 1). Large scale additive manufacturing utilizes a single screw extruder to melt and extruding the pelletized feedstock which increases the flow rate significantly comparing to conventional extrusion-based additive processes. Fiber filled polymer composites are extensively used in large scale AM as to achieve superior material performances.



Figure 1. The Big Area Additive Manufacturing (BAAM) system and products fabricated by BAAM (1).

## MOTIVATION

- Fiber filled polymer composites are extensively applied in large scale additive manufacturing in order to achieve superior material performance and dimensional stability for the outcome products.
- Flow-induced fiber orientation is a key factor in determining the final properties of printed parts, especially when large dimension parts are fabricated. In large scale additive manufacturing,
- The single screw generates unique swirling motion to the flow kinematics which will yield specific pattern of fiber alignment and elastic properties of the printed extrudate.

## OBJECTIVES

- Solve the polymer flow kinematics with realistic rheology model.
- Compute the fiber orientation distribution using weakly coupled method.
- Predicted the elastic properties of a printed extrudate.

## REFERENCES

- 1) <http://www.compositesworld.com/news/2016/01/01/01-additive-manufacturing-patent-agreement>
- 2) <http://www.additive.com/news/2016/01/01/01-additive-manufacturing-patent-agreement>
- 3) Wang, J., Jia, F., Giers, and Charles L. Tucker III. "An objective model for slow orientation kinetics in concentrated fiber suspensions: Theory and rheological evidence." *Journal of Rheology* 52.3 (2008): 1179-1205.
- 4) Jia, David A., and Douglas E. Smith. "Elastic properties of short-fiber polymer composites: derivation and demonstration of analytical forms for expectation and variance from orientation tensors." *Journal of Composite Materials* 42.3 (2008): 271-288.
- 5) V. Kunc, Advances and challenges in large scale polymer additive manufacturing, 15th SPE Automated Composites Conf. Novi, MI (2016).
- 6) Li, L., V. Kunc, D. Rose, C. E. Dury, A. M. Elliott, B. K. Poon, R. J. Smith, C. A. Blue, The importance of carbon fiber to polymer additive manufacturing, *J. Mater. Res.* 29 (2014): 1853-1858.
- 7) Dury, Chad E., et al. "Structure and mechanical behavior of Big Area Additive Manufacturing (BAAM) materials." *Rapid Prototyping Journal* 21 (2017): 141-145.
- 8) <http://www.strangress.com/>

2018 Society of Plastics Engineers Annual Technical Conference

## ABSTRACT

- Effects of single screw motion on predicted fiber orientation of a printed extrudate are investigated.
- Finite element modeling of the melt flow based on the Strangress Model 19 large scale additive manufacturing extruder, including the screw ending part, the extrusion nozzle part and a short section of free extrudate.
- The distance between screw tip and nozzle inlet is of special interest, which is expected to yield different fiber alignment.
- The Isotropic Rotary Diffusion (IRD) model, the Reduced Strain Closure (RSC) model are applied in fiber orientation computation.



Figure 3. Evolution of Fiber Filled Fabrication system from small scale to large scale rapid prototyping.

## FLOW MODELING

The polymer melt flow kinematics is solved by the finite element suite ANSYS Polyflow. The flow rate at the inlet is  $4 \times 10^{-7} m^3/s$ , which resulting in a peak shear rate around  $100 s^{-1}$  at nozzle exit. Rheology properties 13% wt. carbon fiber filled ABS are measured and fitted in a six-mode Phan-Thien-Tanner (PTT) model.

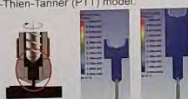


Figure 4. Screw nozzle flow modeling in ANSYS Polyflow.

For an incompressible flow under isothermal condition, we have

- conservations of momentum and mass written as
- conservations of momentum:  $-\nabla p + \nabla \cdot \tau + f = \rho a$ ,
- conservations of mass:  $\nabla \cdot v = 0$ ,

where  $T = T_1 + T_2$ , and  $T_2 = 2\tau_2 D$ .

The constitutive equation for the PTT model

$$\exp\left(\frac{\alpha}{\tau_1} \text{tr}(\tau_1)\right) \tau_1 + \lambda \left( \left(1 - \frac{\alpha}{2}\right) \tau_1 + \frac{\alpha}{2} \tau_1^2 \right) = 2\tau_1 D$$

where  $\tau_1^2 = \frac{\partial \tau_1}{\partial t} + \tau_1 \cdot (\nabla v)^T + (\nabla v) \cdot \tau_1$

$$\tau_1^T = \frac{\partial \tau_1}{\partial t} - \tau_1 \cdot (\nabla v)^T - \tau_1 \cdot D + \frac{1}{2}((\nabla v) + (\nabla v)^T)$$

SPE Poster Number: 2018-G20



BAYLOR  
UNIVERSITY

## FIBER ORIENTATION COMPUTATION

To better characterize the variation of the swirling motion along the extrusion flow, two fiber orientation models are considered (e.g. Isotropic Rotary Diffusion (IRD), and Reduced Strain Closure (RSC) models).

- Isotropic Rotary Diffusion (IRD) model\* [2]

$$A = \frac{\partial A}{\partial t} + v \cdot \nabla A = W \cdot A - A \cdot W + \zeta(D \cdot A + A \cdot D - 2A \cdot D) + 2C_f(I - 3A)$$

- Reduced Strain Closure (RSC) model\* [2]

$$A = \frac{\partial A}{\partial t} + v \cdot \nabla A = W \cdot A - A \cdot W + \zeta(D \cdot A + A \cdot D - 2(A + (1 - \kappa)(L - M(A); D) + 2\kappa C_f(I - 3A))$$

\*More detail of the models can be found in cited literature [2]

## RESULTS

The weakly coupled formulation is applied in evaluating the fiber orientation tensor. We assume isotropic fiber alignment at the flow inlet as the initial condition for the fiber orientation computation.

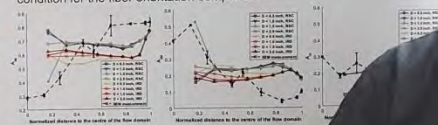


Figure 6. Steady state fiber orientation at the cross-section of a printed extrudate.

Furthermore, by employing the Tandon-Wang method, averaged elastic properties of a printed extrudate based on fiber orientation tensors.

Table 2. Predicted Averaged elastic properties of a extrudate based on fiber orientation tensors.

1D model	Applied model	$E$	$\nu$	$G$	$\nu$	$E$	$\nu$	$G$	$\nu$	$E$	$\nu$	$G$	$\nu$
2.2	IRD	30	0.15	1.13	3.40	7.08	0.15	3.40	7.08	30	0.15	3.40	7.08
2.6	RSC	30	0.15	1.13	3.40	7.72	0.15	3.40	7.72	30	0.15	3.40	7.72
1.5	IRD	30	0.15	1.13	3.41	7.62	0.15	3.41	7.62	30	0.15	3.41	7.62
1.5	RSC	30	0.15	1.13	3.40	7.86	0.15	3.40	7.86	30	0.15	3.40	7.86
1.8	IRD	30	0.15	1.13	3.40	7.51	0.15	3.40	7.51	30	0.15	3.40	7.51
1.8	RSC	30	0.15	1.13	3.40	7.59	0.15	3.40	7.59	30	0.15	3.40	7.59
0.5	IRD	30	0.15	1.13	3.38	7.22	0.15	3.38	7.22	30	0.15	3.38	7.22
0.5	RSC	30	0.15	1.13	3.38	7.22	0.15	3.38	7.22	30	0.15	3.38	7.22

\*Note: 1D refers to the 1D model, 2D refers to the 2D model, 3D refers to the 3D model.

Table 2. Base material properties used in the estimation.

Material	$E$ (GPa)	$\nu$	$G$ (GPa)	$\nu$
Carbon fiber	234	0.2	1.13	3.40
ABS matrix	2.1	0.35	0.68	0.2

\*Note: 1D refers to the 1D model, 2D refers to the 2D model, 3D refers to the 3D model.

Table 3. The base material properties used in the estimation.

Material	$E$ (GPa)	$\nu$	$G$ (GPa)	$\nu$
Carbon fiber	234	0.2	1.13	3.40
ABS matrix	2.1	0.35	0.68	0.2

\*Note: 1D refers to the 1D model, 2D refers to the 2D model, 3D refers to the 3D model.

Table 3. The base material properties used in the estimation.

By considering the swirling kinematics, the numerical results show good agreement with the experimental results.

Different screw ending position changed the degree of anisotropy of transverse fiber orientation than IRD model.

RSC model captures more screw swirling fiber orientation than IRD model.

## ACKNOWLEDGMENTS

The authors would like to thank the Strangress Corporation [7] for donating the Model-19 extruder as well as the financial support offered by Baylor University.

ZHAOGUI WANG  
GRADUATE ASSISTANT  
BAYLOR UNIVERSITY  
WACO TX  
ANTEC  
254892





# STUDY OF VARIATIONS IN MECHANICAL PROPERTIES OF COMPOSITE RAILROAD TIES MADE FROM RECYCLED POLYMERS USING CONSTITUTIVE MODELING

PhD Student: Daniel Pulipati

Advisor: Dr. David Jack

Department of Mechanical Engineering  
Baylor University, Waco, TX

## INTRODUCTION

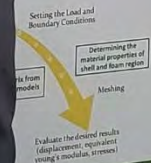
Since the use of railroads in the US began, hardwood timbers were the primary choice for the cross-ties. Wooden cross-ties have a short lifespan and have to be replaced often due to environmental exposure. To increase the lifespan of the cross-ties, preservatives such as creosote are used. Creosote being a hazard, causes skin rashes, lung cancer and various health related issues along with contaminating ground water and affecting plant life. Therefore, various materials such as concrete, steel, and synthetic fiber reinforced composites (as shown in Figure 1 (a)) have been studied as an alternative to wooden ties.

The primary focus of this research is related to the use of recycled polyolefins with fiber reinforcement manufactured with hybrid blow extrusion molding techniques to make cross-ties. HDPE and reinforced GFPP is used along with blowing agents and carbon black to make a cross-tie. The blowing agent is activated under increasing temperature and pressure, which expands and leaves cells (air bubbles) in the core region as shown in Figure 1 (b). The resulting product has a shell region that is nearly solid with few open cells and a foamed core region which contains cells.



## DEFINITIONS

The railroad tie in COMSOL to simulate the tie is modeled using the Young's modulus and other engineering constants and homogenization methods for the shell and core regions. The homogenization methodology is shown in Figure 2. The homogenization and engineering constants calculations are shown in black text.



## ABSTRACT:

The purpose of this research is to predict the material properties and model the behavior of railroad ties fabricated from recycled polymer post-consumer (post-industrial waste), such as HDPE (High Density Polyethylene) and GFPP (Glass Fiber Polypropylene) or similar materials. A commonly employed technique is to fabricate the ties using hybrid blow extrusion molding to produce a foamed core region and a solid shell. The mechanical behavior of railroad ties directly correlates to the volume fraction of the fibers, fiber properties, fiber aspect ratio, fiber orientation and properties of the polymer matrix. Changing any of the aforementioned parameters will affect the final part behavior of the railroad ties. This study will introduce methods to incorporate the variations in shell and the foamed core regions using constitutive models for the locally varying anisotropic stiffness. The stiffness tensor is then used as an input for the shell and foam regions in a Finite Element model to highlight the change in the structural response of the composite tie to variations of the fiber and matrix parameters.

## MATERIAL PROPERTIES AND ASPECT RATIO

The material properties of GFPP and HDPE are obtained from various data sheets and testing. For aspect ratio, the fibers and residue are put into a Scanning Electron Microscope and multiple measurements of the fibers are taken. Lengths were measured at 200x and diameters were measured at 500x magnifications respectively.  $A_{fr}$  was measured to be 25.

Table 1 Material Properties

Parameters	Constituent Values from Data Sheets
Modulus of Matrix	870 MPa
Modulus of Fiber	80 GPa
Poisson's ratio of Matrix	0.45
Poisson's ratio of Fiber	0.23
Aspect Ratio	25
Volume Fraction of Fiber	0.33%

The dimensions of the tie are measured to be  $0.2286 \text{ m} \times 0.1778 \text{ m} \times 1.8288 \text{ m}$  ( $9'' \times 7'' \times 72''$ ). A model was created in COMSOL with a shell region on the outside with a thickness of  $0.01905 \text{ m}$  ( $3/4''$ ) and an inner region with the core as shown in Figure 3.



FIG. 3: (a) Four point bend test (b) The geometry with prescribed forces

## MODELING FOR SHELL AND FOAM MODULUS

Using the material properties and aspect ratio, the stiffness of a unidirectional composite can be calculated using the Voigt-Reuss model. The shear form modulus for random fibers was given by Tucker and Lawrence, and the full form expressed is given by Castejon 2008.

$$A_{fr} = \frac{A_{fr}}{A_{fr}}$$

where  $\mathbf{v}$  is the unit vector and  $\rho(\mathbf{v})$  is the probability density function.

The diagonal components of  $A_{fr}$  describe the amount of fiber alignment in the  $x$ ,  $y$ , and  $z$  directions. The orientation state is assumed to be perfectly random for the random tie, i.e.  $A_{fr} = \frac{1}{3}$ . The homogenized stiffness tensor can be found as functions of the orientation tensor according to the following equations for stiffness (see, e.g. [5]):

$$C_{1111} = A_{fr} C_{11} + A_{fr} C_{22} + A_{fr} C_{33} + A_{fr} C_{44} + A_{fr} C_{55} + A_{fr} C_{66} + A_{fr} C_{77} + A_{fr} C_{88} + A_{fr} C_{99}$$

The four order stiffness tensor calculated is contracted to the second order stiffness tensor. The compliance tensor  $S_{fr}$  is calculated using the inverse of the stiffness tensor. From the compliance tensor the Young's modulus and various engineering constants can be calculated. The obtained result,  $E$ , is the modulus for the shell.  $E$  calculation the modulus of the foam, the Mori-Tanaka method is used.

## PRESENTATION OF DATA AND RESULTS



FIG. 4: (a) Stress-strain curve for a tie. (b) Results from COMSOL, four point bend test simulation. (c) Young's modulus with varying aspect ratio and volume fraction

## CONCLUSIONS

The displacements for the four point bend test and the COMSOL model differ by 0.1 inch and have an error of 1.2%. The stiffness matrix  $C_{fr}$  and engineering constants of the tie can be calculated for varying aspect ratio and foam fraction.

## REFERENCES

- 1. Castejon, J. L. "Mechanical Properties of Randomly Oriented Fiber Reinforced Composites." *Journal of Composite Materials*, vol. 42, no. 1, 2008, pp. 1-15.
- 2. Tucker, R. L., and L. A. Lawrence. "Mechanical Properties of Randomly Oriented Fiber Reinforced Composites." *Journal of Composite Materials*, vol. 42, no. 1, 2008, pp. 1-15.

## ACKNOWLEDGMENTS

We thank Baylor University and Axion Structural Innovations for their financial support.





**ANTEC<sup>®</sup> ORLANDO**  
The Plastics Technology Conference  
May 7-10, 2018 • Orange County Convention Center • Orlando, FL

SPE INSPIRING PLASTICS PROFESSIONALS

# EVALUATING RHEOLOGICAL PROPERTY OF POLYMERS OR POLYMER COMPOSITES DIRECTLY FROM FILAMENTS USED IN FUSED FILAMENT FABRICATION

**Jingdong Chen**  
Advisor: Prof. Douglas E. Smith, Ph.D.  
Department of Mechanical Engineering  
Baylor University, WACO, TX

## BACKGROUND

Generalized Newtonian Fluids  
Purely viscous fluid with shear rate dependent viscosity often used to model polymer melt flow [1]

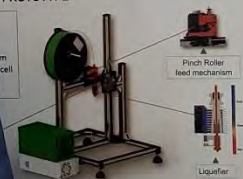
## MOTIVATION:

No method available to directly assess the melt flow rheology of an FFF polymer or polymer composite filament directly

## OBJECTIVE:

Using FFF technology to build a low-cost device capable of measuring the force required to extrude the melted filament through a nozzle, providing pressure drop and a means to compute melt flow rheological property of the filament feedstock.

## PROTOCOL & PROTOTYPE



- Incompressible melt flow
- Melt flow in steady state
- The pressure at the nozzle exit is zero

$$\text{The measured force}$$
$$F = F_{\text{ex}} + F_{\text{nozzle}} \frac{\partial}{\partial x} + F_{\text{ex}} + F_{\text{nozzle}} \frac{\partial}{\partial x}$$
$$F = \Delta P A - F_f$$

Region I:  $\Delta P_1 = 2L_1 \left( \frac{\dot{\gamma}}{2} \right)^n \left( \frac{1}{R_1} \right)^{n+1}$

Region II:  $\Delta P_2 = \frac{4}{3} \cos^2 \left( \frac{\pi}{6} \right) \left( \frac{\dot{\gamma}}{2} \right)^n \left( \frac{1}{R_2} \right)^{n+1} (R_2^{10} - R_1^{10}) [2]$

Region III:  $\Delta P_3 = 2L_3 \left( \frac{\dot{\gamma}}{2} \right)^n \left( \frac{1}{R_3} \right)^{n+1}$

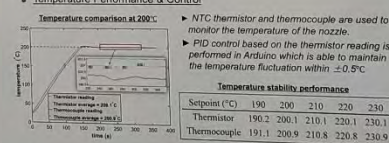
Annual Technical Conference

## ABSTRACT:

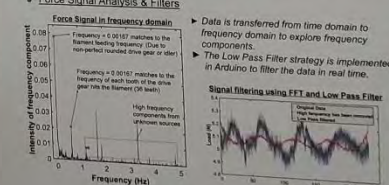
Understanding polymer melt flow behavior is important as it is needed to predict final part quality and improve processing performance, particularly in Fused Filament Fabrication (FFF) additive manufacturing. This work constructed a low-cost device capable of estimating the shear rate dependent viscosity directly from filament feedstock by measuring the force required to extrude a FFF filament through a nozzle. Initial results show that we are able to predict filament melts through a nozzle. Values of consistency index can also be predicted from the measured data with lesser accuracy. This poster describes aspects of the measuring technique and computation of rheology data from measured force. Discrepancies in calculated results are considered in terms of measurement error and the nozzle flow model developed for this study.

## EXPERIMENTAL PREPARATION

### Temperature Performance & Control



### Force Signal Analysis & Filters



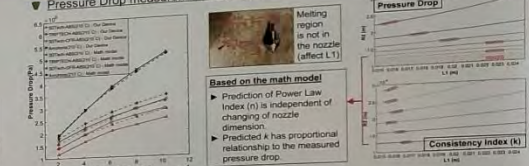
SPE Poster Number: 2018-G19



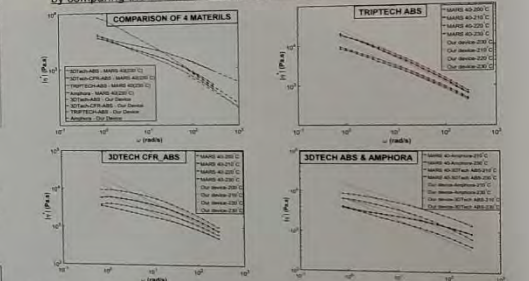
**BAYLOR UNIVERSITY**

## RESULTS & INTERPRETATION

### Pressure Drop measurement & Simulation



The effectiveness of our device on predicting Power Law coefficients are inspected by comparing the data from MARS 40 rheometer



## CONCLUSIONS

- Polymers and polymer composites obey Power Law over shear rate sub-region when processed by FFF technique.
- The Power Law index can be accurately measured using our device for multiple materials at different temperature.
- The difference of pressure drop between measurement and math model mainly comes from the assumption of flow in contraction region. This error is dependent on material and temperature and directly affect the Consistency index prediction.

## FUTURE WORK

- Improve the feed mechanism and structure of the liquefier to minimize the measurement error.
- Implement the Carreau-Yasuda math Model to fit the measured data numerically.
- Customize the nozzle to measure a 'Melt Flow Index' and die swell pressure.

## REFERENCES

- [1] Shaw, M. T., 2012. Introduction to Polymer Rheology, John Wiley & Sons.
- [2] Cogswell, F. N., 1972. 'Converging Flow of Polymer Melts in Extrusion Dies,' Polym. Eng. Sci., 12(1), pp. 64-73.



ANTEC Podium  
Presentation

# Effects of Polymer Rheology on Fiber Orientation in Large-Scale Polymer Additive Manufacturing

Zhaogui Wang

Doctorate Student, Research Assistant  
Mechanical Engineering, Baylor University  
[Zhaogui\\_Wang@baylor.edu](mailto:Zhaogui_Wang@baylor.edu)

Douglas E. Smith, PhD, PE

Associate Professor, Graduate Program Director  
Mechanical Engineering, Baylor University  
[Douglas\\_E\\_Smith@baylor.edu](mailto:Douglas_E_Smith@baylor.edu)

*ANTEC 2018 Orlando*

*May-07-2018*

*09:30 AM – 10:00 AM*







BAYLOR  
UNIVERSITY

# Outreach with other organizations



- Baylor SPE helped host Beach bash at Baylor University
  - SPE talked about various research opportunities available in Baylor Mechanical Engineering.
- Baylor SPE assisted in planning a basketball tournament for the school of Engineering and Computer Science.
  - We partnered with ASME and SWE
  - 50 participants



# Outreach with Community

- Members of Baylor SPE presented at the Hillsboro ISD Career Day
- We taught on the many types and various uses of plastics and did hands on demonstrations with the students.







BAYLOR  
UNIVERSITY

# PlastiVan – McGregor High School



- Baylor SPE chapter organized the PlastiVan event at McGregor High school.
- Over 200 high school students learned about plastics and various engineering opportunities. PlastiVan was sponsored by the SPE composites division.







BAYLOR  
UNIVERSITY

# PlastiVan – Connell Elementary



- Baylor SPE chapter organized the PlastiVan event at Connell Elementary school.
- Over 250 elementary school students learned about plastics and science opportunities. PlastiVan was sponsored by the SPE composites division.







BAYLOR  
UNIVERSITY

# Stepping Out





## May 2017 – September 2018 Purchases



Expenditure	Amount
SPEX Freeze/Mill	\$8,203.25
Grizzly Vertical Mill	\$7,271.33
SPE Polo's	\$80.91
Makerbot and Form 2 supplies	\$671.77
Form 2 cure station	\$700
Food for Meetings	\$491.27
ACCE 2017 Scholarships	\$786.20
Polyolefins Scholarships	\$148.09
ANTEC 2018 Scholarships	\$2075.59
Gas for Facility Tours	\$150.14
NGAB Scholarship	\$113.42
Events	\$13.14
ACCE 2018 Scholarships	\$225.15
<b>Total Expenditures</b>	<b>\$20,580.26</b>





**Thank you for supporting our  
student chapter!**

